REAL-TIME POWER SYSTEM TOPOLOGY CHANGE DETECTION AND IDENTIFICATION

BY

XICHEN JIANG

DISSERTATION

Submitted in partial fulfillment of the requirements
for the degree of Doctor of Philosophy in Electrical and Computer Engineering
in the Graduate College of the
University of Illinois at Urbana-Champaign, 2016

Urbana, Illinois

Doctoral Committee:

Associate Professor Alejandro Domínguez-García, Chair
Professor Peter W. Sauer
Professor Venugopal V. Veeravalli
Assistant Professor Hao Zhu

ABSTRACT

This thesis proposes a framework for detection and identification of system topological changes in near real-time that utilizes the statistical properties of electricity generation and demand, which are assumed to be known. Instead of relying on offline models as with traditional methods, the proposed method is model-free, and exploits the high-speed synchronized measurements provided by phasor measurement units (PMUs). In this framework, a statistical quickest change algorithm is applied to the voltage phase angle measurements collected from PMUs to detect the change-point that corresponds to the system topology change instant. An advantage of this algorithm is that the operator also has full control over the tradeoff between detection delay and false alarm rate. Additionally, a full measurement set is not necessary for its implementation and good results can be achieved even for a few PMU measurements. A scheme for systematic PMU bus selection is presented along with a method to partition the power system such that the aforementioned algorithm for line outage detection can be applied in parallel to each area, allowing for even faster detection. The optimal partitioning scheme is formulated as an integer program and solved using a greedy algorithm.

In the second half of the thesis, an adaptive line outage detection algorithm that accounts for the transient dynamics following a line outage is proposed. A more accurate governor power flow model of the power system is used. This new algorithm is shown to have better performance compared to existing algorithms for line outage detection. In order to lend support for the work done in this thesis, case studies are done through simulations on standard IEEE test systems.

To my parents, Xiaoyun and Haiming.

ACKNOWLEDGMENTS

Throughout my four years of Ph.D. study, I have been immensely blessed with immeasurable support, encouragement, and advice from those around me. Because of this, I am forever grateful. First and foremost, I would like to express my deepest gratitude to my Ph.D. advisor, Professor Alejandro Domínguez-García, for his guidance and support. I could not have been blessed with a better advisor. He cares about each and every one of his students at a personal level and encourages them to conduct research with the highest standards. From him, I learned more than I could ever have asked for.

I would also like to thank Professor Venu Veeravalli, and my fellow graduate students Christine Chen and George Ravatsos, for their collaboration on the research. Their insight was invaluable to the completion of this thesis.

To my family, I thank all of you. Starting from my grandparents (Xie Gao Yang, Gu Qi Min, Li Xia Feng, Jiang Yu Gan), who have supported me since the beginning of this academic journey; they were my biggest fans, cheering me on from the sidelines. I hope the completion of this degree makes all of you proud. To my parents, Haiming and Xiaoyun, who left so much behind and gave up so much for a better life and education here: Thank you so much. You were there for me when I encountered difficulties and there to share the joy of my accomplishments. I am forever grateful to you.

Finally, it was during these tumultuous years of graduate school that I was able to find the love of my life, Qi Li. Her boundless love, uplifting encouragement, and patience for my gripes have brought me the inner peace needed to complete this work. Thank you for allowing me the freedom to fulfill my lifelong dream. Thank you for being my better half and keeping me from having to live out my life in solitude. Thank you for accepting me for who I am. One day in the distant future, when we are both old and gray, I hope to reflect back and see this end of the Ph.D. journey as the start of our wonderful life together.

TABLE OF CONTENTS

CHAPTER 1

INTRODUCTION

In this chapter, we present the motivation for developing algorithms for topological change detection in power systems. This is followed by a survey of prior work published in the area of change detection and PMU placement. We then present the contributions of our research in relation to these topics and outline the rest of the document, concluding with future research directions.

1.1 Motivational Background

Timely line outage detection for power systems is crucial for maintaining operational reliability. Currently, many of the methods for online power system monitoring rely on a system model that is obtained offline, which can be inaccurate due to bad historical or telemetry data; such inaccuracies have been a contributing factor in many recent blackouts. For example, in the 2011 San Diego blackout, operators were unable to determine overloaded lines because the network model was not up to date [1]. This lack of situational awareness limited the operators' ability to identify and prevent the next critical contingency, leading to instability and cascading failures. Similarly, during the 2003 Northeast blackout, operators failed to initiate the correct control schemes because they had an inaccurate model of the system, and could not identify the loss of key transmission elements [2]. These blackouts highlight the importance of developing online techniques to detect and identify system topological changes.

This thesis addresses the problems discussed above by establishing a framework for quickly detecting system topological changes. Specifically, we focus on the problem of line outage detection in power systems, and exploit fast measurements provided by PMUs to develop a statistical method that allows

for quick detection of network topological changes. Additionally, it would not be economical to place a PMU at every bus across the power network. Therefore, we also consider the problem of optimal PMU placement at strategic locations for line outage detection.

1.2 Prior Work

Early approaches for topological change detection and identification include algorithms based on state estimation [3]–[5], and rule-based algorithms that mimic system operator decisions [6]. The issue of external system topology error detection was explored in [7]. More recent proposed methods exploit the fast sampling of voltage magnitudes and phases provided by PMUs to detect events in a power system in near real-time [8]–[11]. While these works allow for improved situational awareness of the power system, they do have shortcomings. Mainly, they do not exploit the fact that the line outage is persistent; i.e., once a line outage occurs, it persists until it is detected and brought back into service. Instead, only the most recent PMU measurement is used to determine if an outage has occurred. The authors of [12] proposed a method to detect line outages using statistical classifiers where a maximum likelihood estimation is performed on the PMU data. The authors also considered the transient response of the system after a line outage by comparing synthesized data against actual data. However, their method requires the exact instant the line outage occurs to be known before applying the algorithm, whereas the method we propose in this paper does not have this restriction.

In [13], [14], the authors proposed a statistical method based on the theory of quickest change detection (QCD) for line outage detection and identification. This method observes a sequence of measured voltage phase angles provided by PMUs and exploits the fact that their statistics change following a line outage. The objective is to detect this change in distribution quickly while subject to a fixed false alarm rate. The statistics of the measured voltage angles pre- and post line outage are related to the known distributions in the real power injections through a linear mapping involving a linearized power flow model. For this method, the incremental changes in real power injections are modeled as independent random variables. Then, the probability distribution of such incremental changes is mapped to that of the

incremental changes in voltage phase angles via a linear transformation obtained from the power flow equations. The PMUs provide a random sequence of voltage phase angle measurements in real-time; when a line outage occurs, the probability distribution of the incremental changes in the voltage phase angles changes abruptly. The objective is to detect a change in this probability distribution after the occurrence of a line outage as quickly as possible while maintaining a desired false alarm rate. In the previous work in [13], [14], the Cumulative Sum (CuSum) algorithm was proposed to solve this problem. For this algorithm, a sequence of CuSum statistics is computed, one for each line in the system. An outage is declared when any one of the statistics crosses a prespecified threshold for the first time. The performance of this algorithm is characterized by a parameter known as the Kullback-Leibler (KL) divergence (see, e.g., [15]), which is a distance measure between the pre- and post-outage voltage phase angle distributions.

Since full PMU placement on every bus could be costly, there has been research on optimal PMU placement at select buses. However, most of the research has been focused on achieving network observability with minimum number of PMUs; on the other hand, the objective of our research is to find the optimal PMU placement for quickly detecting network topological changes. Heuristic techniques for determining optimal placement include simulated annealing, nondominated sorting genetic algorithm, and particle swarm methods [16]–[18]. In [19], the authors also proposed a PMU placement strategy for optimizing a line outage detection scheme. Similar to our work, they formulate the problem as an integer program and then upper and lower bound the optimal solution by using a greedy algorithm and a convex relaxation. Their objective is to maximize the minimum of the voltage phase angle signatures associated with the line outages, where the line outage signatures are based on the pre- and post-outage mean of the phase angles. In contrast, we optimize the PMU placement based on the persistent covariance shift of the voltage phase angles pre- and post-outage. In general, this problem of optimal PMU placement with constraints is an integer programming (IP) problem that is considered NP-hard and may not have a unique solution [20].

1.3 Contributions

This thesis extends the framework introduced in [13], [14] in several directions. We consider the scenario where the power system has a limited number of PMUs deployed instead of requiring the availability of PMUs at all buses. Additionally, we formulate the problem of determining the optimal number of PMUs and their locations while achieving the desired line outage detection performance. We then present a method to partition the power system into smaller subsystems so that the proposed method of quickest change detection for line outages can be applied for each subsystem in parallel. The partitioning algorithm is optimal in the sense that the number of lines within each area is balanced while minimizing the number of tie-lines across areas. We show that by setting the detection threshold scaled according to the so-called Kullback-Leibler (KL) divergence for each line outage, lower detection delay could be achieved.

Finally, we propose an algorithm for line outage detection on the power system that considers the transient response immediately following the line outage. For example, after an outage, the transient behavior of the system is dominated by the inertial response from the generators. This is followed by the governor response and then the automatic generation control (AGC). We incorporate these dynamics into the power system model by relating incremental changes in active power demand to active power generation. We use this model to develop the Dynamic CuSum test (D-CuSum), which is used to capture the transient behavior in the non-composite QCD problem (see e.g., [15], [21]). Then, the Generalized Dynamic CuSum test (G-D-CuSum) is derived by calculating a D-CuSum statistic for each possible line outage scenario; an outage is declared the first time any of the test statistics crosses a pre-specified threshold. The proposed test has better performance because it takes the transient behavior into account in addition to the persistent change in the distribution that results from the outage. To show viability, the proposed algorithms are applied to several IEEE test systems.

1.4 Thesis Organization

This thesis is organized into six chapters; a short summary of each remaining chapter is provided next.

Chapter 2. In this chapter, we provide the preliminary background of this research along with the statement of the problem to be addressed. Specifically, we introduce the power system model and the assumptions we adopt, the pre- and post-outage statistical model of the voltage phase angles, and the problem statement of quickest change detection. Starting from the nonlinear power balance equations, we derive the linearized incremental model of the system and then apply the DC power flow assumptions. The resulting proposed model captures the transient dynamics following a line outage. Finally, the statistical model for the incremental power injections and how they relate to the voltage phase angle statistics are also introduced.

Chapter 3. This chapter outlines the QCD-based line outage identification algorithms, the CuSum algorithm and the Generalized Likelihood Ratio Test algorithm. Small examples are provided to illustrate this process. We also introduce the KL divergence, which is an important measure for characterizing the performance of these detection algorithms. Finally, various other algorithms for line outage detection that exist in the literature are discussed. These algorithms are "one-shot" detection schemes that do not exploit the persistence of the line outage. We compare the performance of our proposed method against those of others and show that the CuSum-based method is better.

Chapter 4. A new line outage algorithm that accounts for the transient dynamics that occur following a line outage on the system is proposed in this chapter. The relation between active power generation and load demand is modeled using participation factors. The improved algorithm is shown to have better performance compared to existing line outage detection algorithms and the algorithm proposed in Chapter 3, where the system transient dynamics are not considered.

Chapter 5. Various extensions of the basic QCD-based algorithm are presented in this chapter. These include partitioning the power system into multiple areas and applying the QCD-based algorithms in parallel for better scalability. In the case where PMUs are limited, a method to determine the optimal PMU allocation for each area is presented. It is shown that both of

these extensions can be formulated as an optimization program. These new concepts are reinforced through case studies.

Chapter 6. This chapter concludes this work by summarizing what has been done as part of this research along with additional insights and remarks. Future research directions are also provided.

CHAPTER 2

PRELIMINARIES

In this chapter, we present the power system model adopted in this research. A linearized small-signal power system model is used in conjunction with synchronized voltage phase angle measurements obtained from phasor measurement units. We provide a general framework where the system transient dynamics after a line outage are captured in the model. We then establish a statistical framework for both the pre- and post-outage scenarios that is used in the line detection algorithm. This chapter concludes with the statement of the line outage detection problem.

2.1 Power System Model

We represent the power system network by a graph consisting of N nodes and L edges, corresponding to buses and transmission lines, respectively. The set of buses is denoted by $\mathcal{V} = \{1, \ldots, N\}$, and the set of transmission lines is denoted by $\mathcal{E}$, where for $m, n \in \mathcal{V}$, $(m, n) \in \mathcal{E}$ if there exists a transmission line between buses m and n. At time t, let $V_i(t)$ and $\theta_i(t)$ denote the voltage magnitude and phase angle at bus i, and let $P_i(t)$ and $Q_i(t)$ denote the net active and reactive power injection at bus i. Then, the quasi-steady-state behavior of the system can be described by the power flow equations, which for bus i can be written as:

$$\begin{aligned} P_i(t) &= p_i(\theta_1(t), \ldots, \theta_N(t), V_1(t), \ldots, V_N(t)), \\ Q_i(t) &= q_i(\theta_1(t), \ldots, \theta_N(t), V_1(t), \ldots, V_N(t)), \end{aligned} \tag{2.1}$$

where the dependence on the system network parameters is implicitly captured by $p_i(\cdot)$ and $q_i(\cdot)$ (see e.g., [22]).

2.1.1 Pre-outage Incremental Power Flow Model

Let $P_i[k] \coloneqq P_i(k\Delta t)$ and $Q_i[k] \coloneqq Q_i(k\Delta t)$, $\Delta t > 0$, $k = 0, 1, 2, \ldots$, denote the k^{th} measurement sample of active and reactive power injections into bus i. Similarly, let $V_i[k]$ and $\theta_i[k]$ denote bus i's k^{th} voltage magnitude and angle measurement sample at $t = k\Delta t$, $k = 0, 1, 2, \ldots$. Furthermore, define variations in voltage magnitudes and phase angles between consecutive sampling times $k\Delta t$ and $(k+1)\Delta t$ as $\Delta V_i[k] \coloneqq V_i[k+1] - V_i[k]$ and $\Delta\theta_i[k] \coloneqq \theta_i[k+1] - \theta_i[k]$, respectively. Similarly, variations in the active and reactive power injections at bus i between two consecutive sampling times are defined as $\Delta P_i[k] = P_i[k+1] - P_i[k]$ and $\Delta Q_i[k] = Q_i[k+1] - Q_i[k]$.

Suppose a solution to the power flow equations exists at $(\theta_i[k], V_i[k], P_i[k], Q_i[k])$, $i = 1, \ldots, N$, such that $p_i(\cdot)$ and $q_i(\cdot)$ in (2.1) are continuously differentiable with respect to all θ_i and V_i at $\theta_i[k]$ and $V_i[k]$, $i = 1, \ldots, N$. Then, assuming that $\Delta\theta_i[k]$ and $\Delta V_i[k]$ are sufficiently small, we can approximate $\Delta P_i[k]$ and $\Delta Q_i[k]$ as

$$\Delta P_i[k] \approx \sum_{j=1}^{N} a_{ij}[k]\Delta\theta_j + \sum_{j=1}^{N} b_{ij}[k]\Delta V_j, \tag{2.2}$$

$$\Delta Q_i[k] \approx \sum_{j=1}^{N} c_{ij}[k]\Delta\theta_j + \sum_{j=1}^{N} d_{ij}[k]\Delta V_j, \tag{2.3}$$

where

$$a_{ij}[k] = \frac{\partial p_i}{\partial \theta_j},\ b_{ij}[k] = \frac{\partial p_i}{\partial V_j},\ c_{ij}[k] = \frac{\partial q_i}{\partial \theta_j},\ d_{ij}[k] = \frac{\partial q_i}{\partial V_j},$$

for each bus $i = 1, \ldots, N$, all evaluated at $(\theta_i[k], V_i[k], P_i[k], Q_i[k])$.

Under standard assumptions used in power system analysis, we assume that $b_{ij} << a_{ij}$ and $c_{ij} << d_{ij}$ in (2.2) and (2.3) [22]. This allows for the decoupling of (2.2) and (2.3) as the variations in the active power injections primarily affect the bus voltage angles; therefore, we can write $\Delta P_i[k] \approx \sum_{j=1}^{N} a_{ij}[k]\Delta\theta_j[k]$. Furthermore, under the so-called DC assumptions, namely (i) the system is lossless, (ii) $V_i[k] = 1$ per unit (p.u.) for all $i \in \mathcal{V}$, k, and (iii) $\theta_m[k] - \theta_n[k] << 1$ for all k and for $m, n \in \mathcal{V}$, $a_{ij}[k]$ simply becomes the negative of the imaginary part of the $(i,j)^{th}$ entry of the network admittance matrix and independent of k [22]. One of the buses must be designated as reference (i.e., $\theta = 0$) for the other buses in the system. There-

fore, since the reference bus angle is assumed to be known, the equation for the reference bus is omitted from (2.2). We can express the variations in the voltage phase angles due to the variations in the real power flow in matrix form by

$$\Delta P[k] \approx H_0 \Delta\theta[k], \tag{2.4}$$

where $\Delta P[k]$, $\Delta\theta[k] \in \mathbb{R}^{(N-1)}$ and $H_0 \in \mathbb{R}^{(N-1)\times(N-1)}$. Note that the $N-1$ dimension of the vectors is the result of omitting the reference bus equation.

In an actual power system, random fluctuations in the load drive the generator response. Therefore, in this work, we use the so-called governor power flow model (see e.g., [23]), which is more realistic than the conventional power flow model, where the slack bus picks up any changes in the load power demand. In the governor power flow model, at time instant k, the relation between changes in the load demand vector, $\Delta P^d[k] \in \mathbb{R}^{N_d}$, and changes in the power generation vector, $\Delta P^g[k] \in \mathbb{R}^{N_g}$, is described by

$$\Delta P^g[k] = B[k]\Delta P^d[k], \tag{2.5}$$

where $B[k]$ is a time dependent matrix of participation factors. We approximate $B[k]$ by quantizing it to take values B_i, $i = 0, 1, \ldots, T$, where i denotes the time period of interest. Let $B[k] = B_0$ and $M_0 \coloneqq H_0^{-1}$ during the pre-outage period. Then, we can substitute (2.5) into (2.4) to obtain a pre-outage relation between the changes in the voltage angles and the real power demand at the load buses as follows:

$$\begin{aligned}
\Delta\theta[k] &\approx M_0 \Delta P[k] \\
&= M_0 \begin{bmatrix} \Delta P^g[k] \\ \Delta P^d[k] \end{bmatrix} \\
&= [M_0^1 \; M_0^2] \begin{bmatrix} B_0 \Delta P^d[k] \\ \Delta P^d[k] \end{bmatrix} \\
&= (M_0^1 B_0 + M_0^2)\Delta P^d[k] \\
&= \tilde{M}_0 \Delta P^d[k],
\end{aligned} \tag{2.6}$$

where $\tilde{M}_0 = M_0^1 B_0 + M_0^2$.

2.1.2 Post-outage Incremental Power Flow Model

Suppose an outage occurs for the line (m, n) at time $t = t_f$, where $\gamma_0 \Delta t \leq t_f < (\gamma_0 + 1)\Delta t$. In addition, assume that the loss of line (m, n) does not cause islands to form in the post-event system (i.e., the underlying graph representing the internal power system remains connected).

Following a line outage, the power system undergoes a transient response governed by B_i, $i = 1, 2, \ldots, T-1$ until quasi steady state is reached, in which $B[k]$ settles to a constant B_T. For example, immediately after the outage occurs, the power system is dominated by the inertial response of the generators, which is then followed by the governor response. As a result of the line outage, the system topology changes, which manifests itself in the matrix H_0. This change in the matrix H_0 resulting from the outage can be expressed as the sum of the pre-outage matrix and a perturbation matrix, $\Delta H_{(m,n)}$, i.e., $H_{(m,n)} = H_0 + \Delta H_{(m,n)}$. Since H_0 has the same sparsity structure as the graph Laplacian of the internal system network, we conclude that the only non-zero terms in the matrix $\Delta H_{(m,n)}$ are $\Delta H_{(m,n)}[n, n] = -\Delta H_{(m,n)}[m, n] = -\Delta H_{(m,n)}[n, m] = \Delta H_{(m,n)}[m, m] = -1/X_{(m,n)}$, where $X_{(m,n)}$ is the imaginary part of the impedance of the outaged line. Thus, the matrix $\Delta H_{(m,n)}$ is a rank-one matrix and can be expressed as

$$\Delta H_{(m,n)} = -\frac{1}{X_{(m,n)}} r_{(m,n)} r_{(m,n)}^T, \tag{2.7}$$

where $r_{(m,n)} \in \mathbb{R}^{N-1}$ is a vector with the m^{th} entry equal to 1, the n^{th} entry equal to -1, and all other entries equal to 0.

We can use the matrix inversion lemma [24] to obtain an expression for $M_{(m,n)} \coloneqq H_{(m,n)}^{-1}$ as follows:

$$M_{(m,n)} = M_0 + \beta_{(m,n)}\ s_{(m,n)}\ s_{(m,n)}^T, \tag{2.8}$$

where $\beta_{(m,n)} = 1/(X_{(m,n)} - r_{(m,n)}^T H_0^{-1} r_{(m,n)})$ and $s_{(m,n)} = H_0^{-1} r_{(m,n)}$.

Then, by letting $M_{(m,n)} \coloneqq H_{(m,n)}^{-1} = [M_{(m,n)}^1\ M_{(m,n)}^2]$, and deriving in the same manner as the pre-outage model of (2.6), we obtain the post-outage relation between the changes in the voltage angles and the real power demand as:

$$\Delta\theta[k] \approx \tilde{M}_{(m,n),i}\Delta P^d[k], \quad \gamma_{i-1} \leq k < \gamma_i, \tag{2.9}$$

where $\tilde{M}_{(m,n),i} = M^1_{(m,n)}B_i + M^2_{(m,n)}$, $i = 1, 2, \ldots, T$.

2.1.3 Instantaneous Change During Outage

At the time of outage, $t = t_f$, there is an instantaneous change in the mean of the voltage phase angle measurements that affects only one incremental sample, namely, $\Delta\theta[\gamma_0] = \theta[\gamma_0 + 1] - \theta[\gamma_0]$. The measurement $\theta[\gamma_0]$ is taken immediately prior to the outage, whereas $\theta[\gamma_0 + 1]$ is the measurement taken immediately after the outage. Then, the effect of an outage in line (m, n) can be modeled with a power injection of $P_{(m,n)}[\gamma_0]$ at bus m and $-P_{(m,n)}[\gamma_0]$ at bus n, where $P_{(m,n)}[\gamma_0]$ is the pre-outage line flow across line (m, n) from m to n. Following a similar approach as the one in [13], the relation between the incremental voltage phase angle at the instant of outage, $\Delta\theta[\gamma_0]$, and the variations in the real power flow can be expressed as:

$$\Delta\theta[\gamma_0] \approx M_0\Delta P[\gamma_0] - P_{(m,n)}[\gamma_0 + 1]M_0 r_{(m,n)}, \tag{2.10}$$

where $r_{(m,n)} \in \mathbb{R}^{N-1}$ is a vector with the $(m-1)^{\text{th}}$ entry equal to 1, the $(n-1)^{\text{th}}$ entry equal to -1, and all other entries equal to 0. Furthermore, by using the governor power flow model of (2.5) and substituting into (2.10), and simplifying, we obtain:

$$\Delta\theta[\gamma_0] \approx \tilde{M}_0\Delta P^d[\gamma_0] - P_{(m,n)}[\gamma_0 + 1]M_0 r_{(m,n)}. \tag{2.11}$$

***Example* 2.1** (Three-Bus System)**.** Consider the lossless three-bus system shown in Fig. 2.1. The parameters for this system are listed in Table 2.1 and all quantities are in per unit. The nonlinear real power balance equations of (2.2) for this system are

$$\begin{aligned}
P_1 &= \frac{V_1V_2}{X_{1,2}}\sin(\theta_1 - \theta_2) + \frac{V_1V_3}{X_{1,3}}\sin(\theta_1 - \theta_3),\\
P_2 &= \frac{V_2V_1}{X_{1,2}}\sin(\theta_2 - \theta_1) + \frac{V_2V_3}{X_{2,3}}\sin(\theta_2 - \theta_3),\\
P_3 &= \frac{V_3V_1}{X_{1,3}}\sin(\theta_3 - \theta_1) + \frac{V_3V_2}{X_{2,3}}\sin(\theta_3 - \theta_2).
\end{aligned} \tag{2.12}$$

Table 2.1: Parameter values for 3-bus system shown in Fig. 2.1.

P_2	P_3	$X_{1,2}$	$X_{2,3}$	$X_{1,3}$
-1	-0.9	0.0504	0.0372	0.0636

The first equation with P_1 is removed from (2.12) since bus 1 is the reference bus. Then, using the DC assumptions, the model of (2.12) can be approximated by a small-signal linear incremental model of the form in (2.4), where

$$\begin{aligned} H_0 &= \begin{bmatrix} \frac{1}{X_{1,2}} + \frac{1}{X_{2,3}} & -\frac{1}{X_{2,3}} \\ -\frac{1}{X_{2,3}} & \frac{1}{X_{1,3}} + \frac{1}{X_{2,3}} \end{bmatrix} \\ &= \begin{bmatrix} 46.72 & -26.88 \\ -26.88 & 42.60 \end{bmatrix}. \end{aligned}$$

Accordingly, $M_0 = H_0^{-1}$ is computed as:

$$M_0 = \begin{bmatrix} 0.033 & 0.021 \\ 0.021 & 0.037 \end{bmatrix}.$$

Suppose an outage occurs on line $(1, 2)$. Then, according to (2.7) and (2.8),

$$\begin{aligned} \Delta H_{(1,2)} &= -\frac{1}{0.0504}[-1, 0]^T[-1, 0] \\ &= \begin{bmatrix} 19.84 & 0 \\ 0 & 0 \end{bmatrix}, \end{aligned}$$

and

$$\begin{aligned} \Delta M_{(1,2)} &= 59.53[-0.033, -0.021]^T[-0.033, -0.021] \\ &= \begin{bmatrix} 0.067 & 0.042 \\ 0.042 & 0.026 \end{bmatrix}. \end{aligned}$$

□

2.2 Measurement Model

Since the voltage phase angles, $\theta[k]$, are assumed to be measured by PMUs, we allow for the scenario where the angles are measured at only a subset of

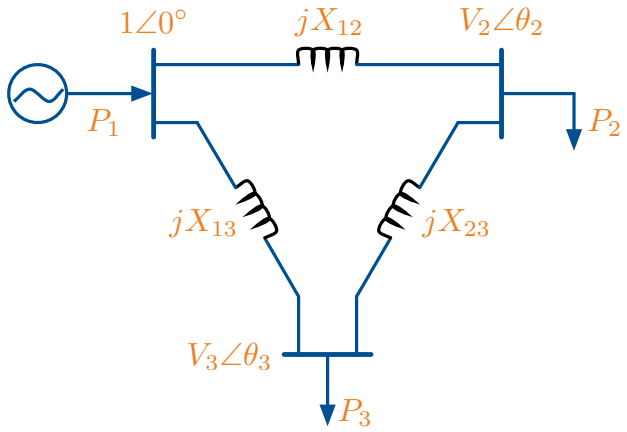

Figure 2.1: Network topology for 3-bus system.

the load buses, and denote this reduced measurement set by $\hat{\theta}[k]$. Suppose that there are N_d load buses and we select $p \leq N_d$ locations to deploy the PMUs. Then, there are $\binom{N_d}{p}$ possible locations to place the PMUs. Let

$$\tilde{M} = \begin{cases} \tilde{M}_0, \text{ if } 1 \leq k < \gamma_0, \\ \vdots \\ \tilde{M}_{(m,n),T}, \text{ if } k \geq \gamma_T. \end{cases} \tag{2.13}$$

Then, the absence of a PMU at bus i corresponds to removing the i^{th} row of $\tilde{M}$. Thus, let $\hat{M} \in \mathbb{R}^{p \times N_d}$ be the matrix obtained by removing $N - p - 1$ rows from $\tilde{M}$. Therefore, we can relate $\hat{M}$ to $\tilde{M}$ in (2.13) as follows:

$$\hat{M} = C\tilde{M}, \tag{2.14}$$

where $C \in \mathbb{R}^{p \times (N-1)}$ is a matrix of 1's and 0's that appropriately selects the rows of $\tilde{M}$. Accordingly, the increments in the phase angle can be expressed as follows:

$$\Delta\hat{\theta}[k] \approx \hat{M}\Delta P^d[k]. \tag{2.15}$$

The small variations in the real power injections at the load buses, $\Delta P^d[k]$, can be attributed to random fluctuations in electricity consumption. In this regard, we may model the $\Delta P^d[k]$'s as independent and identically distributed (i.i.d.) random vectors. By the Central Limit Theorem [25], it can be shown that each $\Delta P^d[k]$ is a Gaussian vector, i.e., $\Delta P^d[k] \sim \mathcal{N}(0, \Lambda)$,

where Λ is the covariance matrix. Note that the elements $\Delta P^d[k]$ need not be independent. Since $\Delta\hat{\theta}[k]$ depends on $\Delta P^d[k]$ through the linear relationship given in (2.15), we have that:

$$\Delta\hat{\theta}[k] \sim \begin{cases} f_0 \coloneqq \mathcal{N}(0, \hat{M}_0 \Lambda \hat{M}_0^T), \text{ if } 1 \leq k < \gamma_0, \\ f_{(m,n)}^{(0)} \coloneqq \mathcal{N}(-P_{(m,n)}[\gamma_0 + 1] C M_0 r_{(m,n)}, \\ \qquad\qquad \hat{M}_0 \Lambda \hat{M}_0^T), \text{ if } k = \gamma_0, \\ \vdots \\ f_{(m,n)}^{(T)} \coloneqq \mathcal{N}(0, \hat{M}_{(m,n),T} \Lambda \hat{M}_{(m,n),T}^T), \text{ if } k \geq \gamma_T, \end{cases} \tag{2.16}$$

It is important to note that for $\mathcal{N}\left(0, \hat{M}\Lambda\hat{M}^T\right)$ to be a nondegenerate p.d.f., its covariance matrix, $\hat{M}\Lambda\hat{M}^T$, must be full rank. We enforce this by ensuring that the number of PMUs allocated, p, is less than or equal to the number of load buses, N_d.

2.3 Problem Statement

Our goal is to detect the change in the probability distribution of the sequence $\{\Delta\hat{\theta}[k]\}_{k\geq 1}$ (that results from the line outage) as quickly as possible while maintaining a certain level of detection accuracy, which is related to, e.g., the false alarm rate. This problem, referred to as quickest change detection (QCD), has been well studied in the statistical signal processing literature. Next, we provide a precise mathematical description of the QCD problem and an algorithm that we will use to detect a line outage; we refer the reader to [21]-[26] for a survey of the theory of QCD and algorithms.

We assume that the sequence $\{\Delta\hat{\theta}[k]\}_{k\geq 1}$ of random vectors is available from PMU measurements. For the base case where no line outages are present, we have that $\Delta\hat{\theta}[k] \sim f_0$. At some random time, t_f, an outage occurs on line (m, n). Then, the pdf of the sequence $\{\Delta\hat{\theta}[k]\}$ changes from f_0 to $f_{(m,n)}^{(0)}$. Then, the system undergoes a series of transient responses which corresponds to the distribution of $\Delta\hat{\theta}[k]$ evolving from $f_{(m,n)}^{(0)}$ to $f_{(m,n)}^{(T)}$. First, a meanshift takes place during the instant of change t_f, where the pdf is $f_{(m,n)}^{(0)}$. Then, the statistical behavior of the process is characterized by a series of changes only in the covariance matrix of the measurements. The

objective is to detect this transition in the pdf of $\{\Delta\hat{\theta}[k]\}$ as quickly as possible. Mathematically, when a line outage occurs, the objective is to find the optimal stopping time τ on the sequence of observations for $\Delta\hat{\theta}$. In the absence of a change, the expectation of τ, $\mathbb{E}[\tau]$, should be maximized so as to avoid false alarms. On the other hand, once a line outage occurs, we expect $\mathbb{E}[\tau]$ to be as small as possible. A formulation that captures this trade-off is as follows [27]:

$$\begin{aligned} &\min_{\tau} \quad \sup_{\gamma_0 \geq 1} \mathbb{E}_{\gamma_0}[\tau - \gamma_0 | \tau \geq \gamma_0] \\ &\text{subject to } \mathbb{E}_{\infty}[\tau] \geq \beta, \end{aligned} \tag{2.17}$$

where $\mathbb{E}_{\gamma_0}$ denotes the expectation with respect to probability measure when a change occurs at time sample γ_0, $\mathbb{E}_{\infty}$ denotes the corresponding expectation when the change never occurs, and $\beta > 0$ is the given constraint on the mean time to false alarm.

2.4 Summary

This chapter set up the framework for the proposed line outage detection and identification method that is to be developed in this work. An incremental DC-like power flow model was derived along with the statistical model for the voltage phase angles, the measurements of which are assumed to be provided by PMUs. In the derivation of the statistical model, we assumed that the incremental variations in the active power injections at each load bus are independent random variables and that the generators react to the changes in these load demands.

CHAPTER 3

LINE OUTAGE IDENTIFICATION: NO TRANSIENTS

This chapter begins by introducing the CuSum algorithm for change detection for the case where only the meanshift and the quasi steady state period following a line outage is considered. This is followed by the presentation of the Kullback-Leibler (KL) divergence, which is an important measure characterizing the distance between two probability distributions; the detection algorithms we present are based on this measure. Then, we introduce the Generalized Likelihood Ratio Test (GLRT) algorithm, which serves as a basis for our line-outage detection method. The performance of the proposed algorithm is compared against other existing line outage detection algorithms in the literature. We show that our algorithm performs better as it exploits the statistical properties of the measured voltage phase angles before, during, and after a line outage, whereas other methods in the literature only utilize the change in statistics that occurs at the instant of outage.

3.1 CuSum Algorithm

Recall the measurement model in (2.16) for the case where $T = 1$:

$$\Delta\hat{\theta}[k] \sim \begin{cases} f_0 \coloneqq \mathcal{N}(0, \hat{M}_0 \Lambda \hat{M}_0^T), \text{ if } 1 \leq k < \gamma_0, \\ f_{(m,n)}^{(0)} \coloneqq \mathcal{N}(-P_{(m,n)}[\gamma_0 + 1] C M_0 r_{(m,n)}, \\ \qquad\qquad \hat{M}_0 \Lambda \hat{M}_0^T), \text{ if } k = \gamma_0, \\ f_{(m,n)}^{(1)} \coloneqq \mathcal{N}(0, \hat{M}_{(m,n),T} \Lambda \hat{M}_{(m,n),T}^T), \text{ if } k \geq \gamma_1. \end{cases} \tag{3.1}$$

Suppose that the p.d.f.'s f_0, $f_{(m,n)}^{(0)}$, and $f_{(m,n)}^{(1)}$, are known. Then, one particular algorithm that possesses the optimality properties with respect to the formulation in (2.17) is the Cumulative Sum (CuSum) algorithm [28]. From the sequence of phase angle measurements, the CuSum algorithm computes a sequence of statistics recursively so that for $k \geq 0$, the statistic $W_{(m,n)}^{\text{CU}}[k+1]$

is computed as

$$W^{\mathrm{CU}}_{(m,n)}[k+1] = \max\left\{ W^{\mathrm{CU}}_{(m,n)}[k] + \log\frac{f^{(1)}_{(m,n)}(\Delta\hat{\theta}[k+1])}{f_0(\Delta\hat{\theta}[k+1])}, \log\frac{f^{(0)}_{(m,n)}(\Delta\hat{\theta}[k+1])}{f_0(\Delta\hat{\theta}[k+1])}, 0 \right\}, \tag{3.2}$$

where $W^{\mathrm{CU}}_{(m,n)}[0] = 0$ for all $(m,n) \in \mathcal{E}$. Denote τ_C to be the time at which the CuSum algorithm declares a line outage; then,

$$\tau_{\mathrm{C}} = \inf\{k \geq 1 : W^{\mathrm{CU}}_{(m,n)}[k] > A^{\mathrm{CU}}_{(m,n)}\}, \tag{3.3}$$

where $A^{\mathrm{CU}}_{(m,n)}$ is a threshold selected for the corresponding $W^{\mathrm{CU}}_{(m,n)}[k]$ statistic. An optimal method to select this threshold will be presented in Section 3.3.

3.2 Generalized Likelihood Ratio Test Algorithm

In the setting we consider for this thesis, since the line for which an outage occurs is unknown, the post-change pdf of $\Delta\hat{\theta}$ is also unknown. However, since the single-line outage can occur in at most L ways, the post-change distribution is known to belong to the finite set $\{f_{(m,n)}, (m,n) \in \mathcal{E}\}$. In this context, we can apply the Generalized Likelihood Ratio Test (GLRT) algorithm where we compute L CuSum statistics in parallel, one for each post-change scenario, and declare an outage the first time a change is detected in any one of the parallel CuSum tests. In other words, we compute (3.2) for each line (m,n) in the system, with $W^{\mathrm{CU}}_{(m,n)}[0] = 0$, and stop at

$$\tau^{\mathrm{CU}} = \inf\left\{ k \geq 1 : \max_{(m,n)\in\mathcal{E}} W^{\mathrm{CU}}_{(m,n)}[k] > A^{\mathrm{CU}}_{(m,n)} \right\}. \tag{3.4}$$

In [13], a single threshold $A^{\mathrm{CU}}_{(m,n)}$ was chosen for all line outage streams $W^{\mathrm{CU}}_{(m,n)}$. However, faster detection can be achieved by choosing an individual threshold $A^{\mathrm{CU}}_{(m,n)}$ for each $W^{\mathrm{CU}}_{(m,n)}$ that is proportional to its corresponding KL divergence. The threshold $A^{\mathrm{CU}}_{(m,n)}$ can be chosen to control the mean time to false alarm; if a larger mean time to false alarm is required, then $A^{\mathrm{CU}}_{(m,n)}$ is set to a larger value, and vice-versa. Finally, this algorithm also identifies the line

that is outaged at τ^{CU} to be

$$(\hat{m}, \hat{n}) = \arg\max_{(m,n)\in\mathcal{E}} W^{\mathrm{CU}}_{(m,n)}[\tau^{\mathrm{CU}}]. \tag{3.5}$$

3.3 Threshold Selection

We now present ways of choosing the thresholds for the CuSum test. It can be shown (see, e.g., [29]) that by choosing

$$A^{\mathrm{CU}}_{(m,n)} = \log\gamma - \log\beta_{(m,n)}, \tag{3.6}$$

with $\beta_{(m,n)}$ being a positive constant independent of γ, the expected delay for each possible outage differs from the corresponding minimum delay among the class of stopping times $\mathcal{C}_\gamma = \{\tau : \mathbb{E}_0(\tau) \geq \gamma\}$, as $\gamma \to \infty$, by a bounded constant.

A choice of thresholds for the CuSum algorithm is obtained by setting $\beta_{(m,n)} = \frac{1}{L}$ for all $(m,n) \in \mathcal{E}$. This way we get a common threshold, i.e., $A^{\mathrm{CU}}_{(m,n)} = A^{\mathrm{CU}} = \log(\gamma L)$ for all $(m,n) \in \mathcal{E}$. It can be shown (see, e.g., [30]) that by choosing the thresholds this way, we can guarantee that $\mathbb{E}_0[\tau^{\mathrm{CU}}] \geq \gamma$.

Using the results in [29], another choice of the thresholds could be based on a relative performance loss criterion, i.e.,

$$\beta_{(m,n)} = \frac{1}{D(f^{(1)}_{(m,n)} \parallel f_0)L(\zeta_{(m,n)})^2)}, \tag{3.7}$$

where

$$\zeta_{(m,n)} = \lim_{b\to\infty} \mathbb{E}^{(1)}_{(m,n)}\left[e^{\{-(S_{(m,n)}[\tau^{\mathrm{b}}_{(m,n)}]-b)\}}\right], \tag{3.8}$$

with

$$\tau^{\mathrm{b}}_{(m,n)} = \inf\{k \geq 1 : S_{(m,n)}[k] \geq b\}, \tag{3.9}$$

and

$$S_{(m,n)}[k] = \sum_{l=1}^{k} \log\frac{f^{(1)}_{(m,n)}(\Delta\hat{\theta}[l])}{f_0(\Delta\hat{\theta}[l])}. \tag{3.10}$$

This choice of threshold depends on the asymptotic overshoot of an Sequential Probability Ratio Test (SPRT)-based test, which is often used in hypothesis testing [15]. As we show through case studies, these thresholds result in

performance gains.

3.4 Intuition Behind the Operation of the GLRT Algorithm

The algorithm we presented in (3.2) for line outage detection is based on the Kullback-Leibler (KL) divergence, which for any two probability densities f and g is defined as follows:

$$D(f \parallel g) := \int f(x) \log \frac{f(x)}{g(x)} dx \geq 0, \tag{3.11}$$

with equality if and only if $f = g$ almost surely. In the context of the line outage detection problem, for an outage of line (m, n), the KL divergence is

$$D(f^{(1)}_{(m,n)} \parallel f_0) = \mathbb{E}\left[\log \left(\frac{f^{(1)}_{(m,n)}(\Delta\hat{\theta}[k])}{f_0(\Delta\hat{\theta}[k])} \right) \middle| (m,n) \text{ outage} \right], \tag{3.12}$$

which provides a bound on the delay for detecting an outage in line (m, n); a larger KL divergence results in lower detection delay and vice versa. Prior to any changes, the mean of the log likelihood ratio is negative due to (3.11). Therefore, $W^{\text{CU}}_{(m,n)}[k]$ would remain close to or at 0 prior to a line outage. On the other hand, after an outage occurs, the mean of the log-likelihood ratio is positive. As a result, $W^{\text{CU}}_{(m,n)}[k]$ increases unboundedly after the outage in line (m, n), and the CuSum algorithm in (3.2) declares the occurrence of an outage in line (m, n) the first time that $W^{\text{CU}}_{(m,n)}[k]$ reaches $A^{\text{CU}}_{(m,n)}$.

In addition, We can use (3.11) to obtain bounds on the false isolation rates. Consider an outage of line (m, n); if $\mathbb{E}\left[\log\left(\frac{f^{(1)}_{(k,l)}}{f_0}\right)\right]$ is positive, then $W^{\text{CU}}_{(k,l)}[k]$ would increase despite no outage in line (k, l). Hence, we would like $\mathbb{E}\left[\log\left(\frac{f^{(1)}_{(m,n)}}{f^{(1)}_{(k,l)}}\right)\right]$ to be maximized so that the false isolation rate for line (m, n) outage is minimized. For example, we can compute $D(f^{(1)}_{(m,n)} \parallel f^{(1)}_{(k,l)})$ to estimate a bound on the false isolation rate, where a small value indicates that an outage in line (k, l) causes a statistical change in the voltage phase angles that is very similar to that corresponding to an outage in line (m, n).

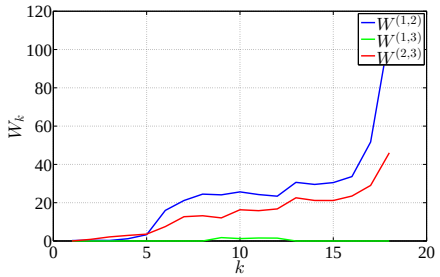

(a) Line $(1, 2)$ outage.

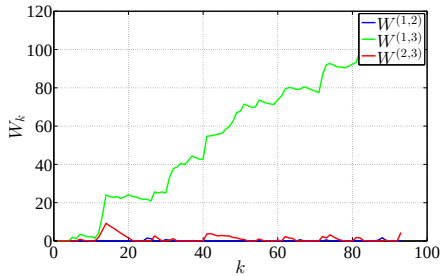

(b) Line $(1, 3)$ outage.

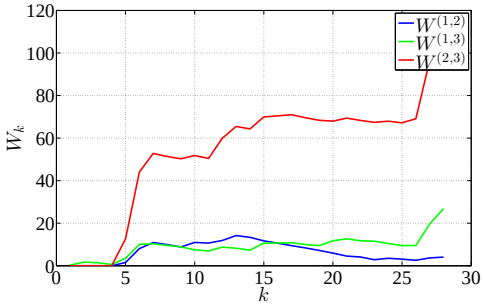

(c) Line $(2, 3)$ outage.

Figure 3.1: Realizations of $W^{\text{CU}}_{(m,n)}[k]$ for each line outage of 3-bus system with PMU at buses 2 and 3.

An extreme case of $D(f^{(1)}_{(m,n)} \parallel f^{(1)}_{(k,l)}) = 0$ occurs when lines (k, l) and (m, n) have the same impedance and share the same terminal buses, i.e., $k = m$, $l = n$. In this case, our algorithm cannot distinguish between the occurrence of an outage on either of the two lines. Next, we illustrate these ideas in a small power system example.

***Example* 3.1** (Three-Bus System)**.** Consider the 3-bus system shown in Fig. 2.1. We apply the GLRT algorithm to detect and identify a line $(2, 3)$ outage at $\gamma_0 = 1$. The PMU measurements are simulated by creating an active power injection time-series data for each load bus i with

$$P_i[k] = P_i[k-1] + v_i, \tag{3.13}$$

where $P_i[0]$ is the nominal power injection at load bus i at instant k, and $v_i \sim \mathcal{N}(0, 0.5)$ is a pseudorandom value representing random fluctuations in electricity consumption. For each set of bus injection data, we solve the nonlinear power flow equations in (2.1) to obtain the sequence of phase angle "measurements" $\{\hat{\theta}[k]\}$. In this example, we assume that bus 1 is the refer-

Table 3.1: 3-bus system KL Div.

KL Div. \ Line Outage (m,n)	$(1,2)$	$(1,3)$	$(2,3)$
$\mathbb{E}\left[\log\left(\frac{f_{(1,2)}}{f_0}\right) \middle\| (m,n) \text{ outage}\right]$	3.69	-1.09	0.75
$\mathbb{E}\left[\log\left(\frac{f_{(1,3)}}{f_0}\right) \middle\| (m,n) \text{ outage}\right]$	-0.86	1.77	1.34
$\mathbb{E}\left[\log\left(\frac{f_{(2,3)}}{f_0}\right) \middle\| (m,n) \text{ outage}\right]$	0.59	-0.02	6.42

ence bus and the random fluctuations at buses 2 and 3 are uncorrelated, so Λ is a diagonal matrix.

Using the GLRT-based algorithm, we execute three CuSum tests in parallel and compute each $W^{\text{CU}}_{(m,n)}[k]$ defined in (3.2), one for each line of the system. Figure 3.1 shows the typical progressions of $W^{\text{CU}}_{(m,n)}[k]$ for each line outage of the 3-bus system. In Fig. 3.1(a), $W^{\text{CU}}_{(1,2)}[k]$ crosses the threshold of $A = 100$ first, while $W^{\text{CU}}_{(1,3)}[k]$ and $W^{\text{CU}}_{(2,3)}[k]$ remain close to 0. Therefore, the algorithm was able to correctly detect and identify the line outage after $k = 25$ samples. Similar behavior was observed for outages of line (1,3) and (2,3). In addition to the plots, Table 3.1 shows the computed KL divergences of all line outages according to (3.11). For example, a positive $\mathbb{E}\left[\log\left(\frac{f_{(1,2)}}{f_0}\right)\middle|(1,2) \text{ outage}\right]$ value of 3.69 means that in the long run, if the outage were indeed on line $(1,2)$, $W^{\text{CU}}_{(1,2)}[k]$ will increase; the rate of this increase depends on the magnitude of the KL divergence. Since $\mathbb{E}\left[\log\left(\frac{f_{(1,2)}}{f_0}\right)\middle|(1,2) \text{ outage}\right] > \mathbb{E}\left[\log\left(\frac{f_{(1,3)}}{f_0}\right)\middle|(1,3) \text{ outage}\right]$, on average, $W^{\text{CU}}_{(1,2)}[k]$ reaches the threshold A in less samples than $W^{\text{CU}}_{(1,3)}[k]$ for an outage of their respective lines. On the other hand, the negative value of $\mathbb{E}\left[\log\left(\frac{f_{(1,2)}}{f_0}\right)\middle|(1,3) \text{ outage}\right]$ means that $W^{\text{CU}}_{(1,2)}[k]$ tends to stay near 0 for a line $(1,3)$ outage, which is observed in Fig. 3.1(b). □

3.5 Other Statistical Algorithms for Power System Line Outage Detection

This section introduces some of the other algorithms that are used for change detection. Specifically, we introduce the meanshift and Shewhart tests, which only consider the latest sample of the voltage phase angles instead of using all of the samples. For example, the line outage detection algorithm proposed

in [8] can be shown to be equivalent to a log-likelihood ratio test that only uses the most recent measurements.

3.5.1 Meanshift Test

The meanshift test is a "one-shot" detection scheme in that the algorithm uses only the most recent observation to decide whether a change in the mean has occurred and ignores all past observations. The meanshift statistic corresponding to line (m, n) is defined as follows:

$$W^{\mathrm{MS}}_{(m,n)}[k] = \log \frac{f^{(1)}_{(m,n)}(\Delta\hat{\theta}[k])}{f_0(\Delta\hat{\theta}[k])}. \tag{3.14}$$

The decision maker declares a change when one of the $|\mathcal{E}|$ statistics crosses a corresponding threshold, $A^{\mathrm{MS}}_{(m,n)}$. The stopping time for this algorithm is defined as:

$$\tau^{\mathrm{MS}} = \inf_{(m,n)\in\mathcal{E}} \left\{ \inf\{k \geq 1 : W^{\mathrm{MS}}_{(m,n)}[k] > A^{\mathrm{MS}}_{(m,n)}\} \right\}. \tag{3.15}$$

The meanshift test ignores the persistent covariance change that occurs after the outage. In particular, note that the meanshift test is using the likelihood ratio between the distribution of the observations before and at the changepoint. More specifically, assuming that an outage occurs in line (m, n), the expected value of the statistic at the changepoint is given by

$$\mathbb{E}^{(0)}_{(m,n)}\left[\log \frac{f^{(0)}_{(m,n)}(\Delta\hat{\theta}[k])}{f_0(\Delta\hat{\theta}[k])} \right] = D(f^{(0)}_{(m,n)} \parallel f_0) > 0. \tag{3.16}$$

On the other hand, after the changepoint ($k > \lambda_0$), the expected value of the statistic is given by

$$\begin{aligned} \mathbb{E}^{(1)}_{(m,n)}\left[\log \frac{f^{(0)}_{(m,n)}(\Delta\hat{\theta}[k])}{f_0(\Delta\hat{\theta}[k])} \right] = \\ = D(f^{(1)}_{(m,n)} \parallel f_0) - D(f^{(1)}_{(m,n)} \parallel f^{(0)}_{(m,n)}), \end{aligned} \tag{3.17}$$

which could be either positive or negative.

3.5.2 Shewhart Test

Similar to the meanshift test, the Shewhart test is also a "one-shot" detection scheme. This test attempts to detect a change on the observation sequence through the meanshift and the change in the covariance matrix of $\Delta\hat{\theta}[k]$. The Shewhart test statistic for line (m,n) outage is defined as:

$$W^{\mathrm{SH}}_{(m,n)}[k] = \max\left\{\log\frac{f^{(0)}_{(m,n)}(\Delta\hat{\theta}[k])}{f_0(\Delta\hat{\theta}[k])}, \log\frac{f^{(1)}_{(m,n)}(\Delta\hat{\theta}[k])}{f_0(\Delta\hat{\theta}[k])}\right\}, \tag{3.18}$$

where the first log-likelihood ratio is used to detect the meanshift, while the second log-likelihood ratio is used to detect the persistent change in the covariance. The stopping time is:

$$\tau^{\mathrm{SH}} = \inf_{(m,n)\in\mathcal{E}}\left\{\inf\{k \geq 1 : W^{\mathrm{SH}}_{(m,n)}[k] > A^{\mathrm{SH}}_{(m,n)}\}\right\}. \tag{3.19}$$

Since the Shewhart test exploits the covariance change in addition to the meanshift statistic, it should perform better than the meanshift test, at least as the meantime to false alarm goes to infinity, which is verified in the case studies.

3.6 Case Studies

This section provides a case study of the concepts introduced in this chapter on the IEEE 14-bus and 118-bus systems [31]. The importance sampling technique for rare events is also presented. An outage is simulated and the proposed algorithm is used to detect this outage. In addition, we demonstrate the effectiveness of our proposed line outage detection algorithm by comparing against other line outage detection algorithms on the IEEE 14-bus system.

3.6.1 Importance Sampling

Since the meanshift in the voltage phase angles occurs between the sample immediately prior to and after the line outage, it is not persistent. If the meanshift test presented in Section 3.5.1 does not capture the outage exactly

when it occurs, then the likelihood of correctly identifying the outage would be a rare event. This is because the log-likelihood ratio used in the meanshift statistic of (3.14) matches only the meanshift but not the covariance shift that is persistent after a line outage. Therefore, in order to simulate detection delays of the meanshift test, the technique of importance sampling is used.

The usual Monte Carlo method of estimating the average detection delay of the meanshift test is

$$\hat{\tau}^{\mathrm{MS}} := \mathbb{E}[\tau^{\mathrm{MS}}] \approx \frac{1}{N} \sum_{i=1}^{N} \tau_i^{\mathrm{MS}}, \tag{3.20}$$

where N is a large sample size and τ_i^{MS} is the detection delay for the i^{th} sample run. For line (m, n) outage simulation, starting with the second sample after the line outage, the voltage phase angles samples are generated from the probability distribution $f_{(m,n)}^{(1)}$. Therefore, the numerator of (3.14) does not match the distribution from which the samples are generated, making the crossing of threshold rare. In order to use importance sampling, we sample from the distribution $f_{(m,n)}^{(0)}$ instead of $f_{(m,n)}^{(1)}$ for all samples after the outage. We use the fact that

$$\mathbb{E}_{f_{(m,n)}^{(1)}} \left[\log \frac{f_{(m,n)}^{(0)}}{f_0} \right] = \mathbb{E}_{f_{(m,n)}^{(0)}} \left[\log \left(\frac{f_{(m,n)}^{(0)}}{f_0} \right) \frac{f_{(m,n)}^{(1)}}{f_{(m,n)}^{(0)}} \right]. \tag{3.21}$$

We modify the meanshift statistic of (3.14) to

$$W_{(m,n)}^{\mathrm{MS}}[k] = \log \left(\frac{f_{(m,n)}^{(0)}(\Delta\hat{\theta}[k])}{f_0(\Delta\hat{\theta}[k])} \right) \frac{f_{(m,n)}^{(1)}(\Delta\hat{\theta}[k])}{f_{(m,n)}^{(0)}(\Delta\hat{\theta}[k])} \tag{3.22}$$

but with sampling of $\Delta\hat{\theta}[k]$ from the distribution $f_{(m,n)}^{(0)}$ after the line outage instead of $f_{(m,n)}^{(1)}$. We declare the detection of line outage when the statistic crosses the threshold. This method greatly reduces the number of sample paths that must be simulated to estimate the detection delay, resulting in greater efficiency.

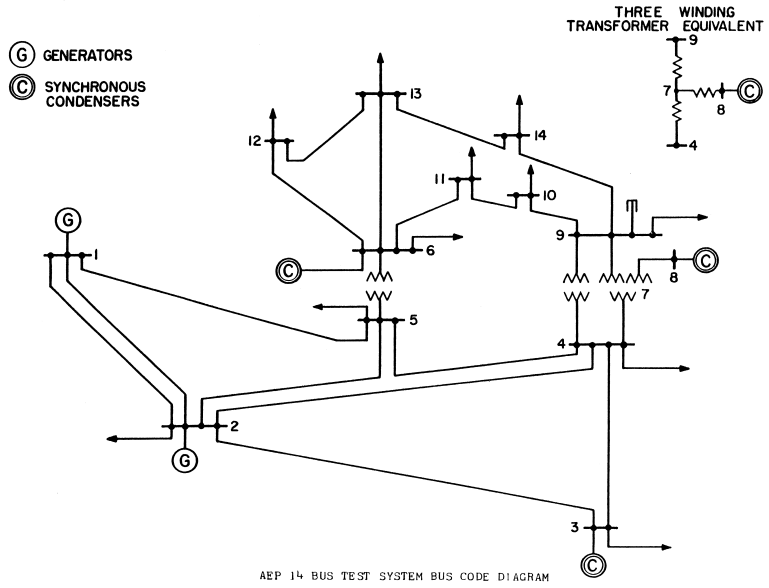

Figure 3.2: Network topology for 14-bus system.

3.6.2 14-Bus System

The one-line diagram of the IEEE 14-bus test system is shown in Fig. 3.2. We simulate a line $(2, 5)$ outage at $k = 10$ and apply the CuSum tests of (3.2) to the voltage phase angle measurements. The random fluctuations in the active power injections are considered independent Gaussian random variables with a variance of 0.03. Therefore, Λ is a diagonal matrix. Figure 3.3 shows that the $W_{(2,5)}[k]$ stream crosses the threshold of 100 before all the other streams at $k = 48$, resulting in a detection delay of 38 samples. Assuming that the PMUs sample voltage angles at a rate of 30 samples per second, the detection delay in this case is about 2 seconds. Again, we see that the streams for the other lines either remain close to 0 or grow at a slower rate than $W_{(2,5)}[k]$.

Next, we perform Monte Carlo simulations for the Shewhart, meanshift, and CuSum algorithms to obtain plots of average detection delay versus mean time to false alarm. The values for the average detection delay are obtained by simulating an outage in line $(4, 5)$ and running the corresponding detection algorithms for different thresholds until a detection of the outaged line is declared. For computing the mean time to false alarm, the detection algorithms are executed for the power system under normal operation until a false alarm occurs. Since false alarm events are in general rare, averaging many

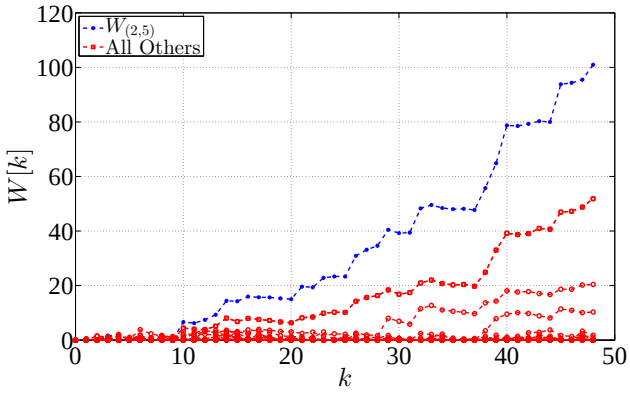

Figure 3.3: Sample run for 14-bus system.

sample runs would incur significant computation time. In order to reduce the simulation time, importance sampling is used for the meanshift and Shewhart tests. For our simulations, we found that the error bounds for all the simulated values are within 5% of the means. Figure 3.4 shows the average detection delay versus mean time to false alarm for all of the detection methods mentioned in this paper. As evidenced by the crossing of the Shewhart and meanshift plots, for small values of mean time to false alarm, the meanshift test performs better than the Shewhart test. It can be verified from QCD theory that the slope of Delay versus log(mean time to false alarm) for the Shewhart and CuSum tests is given by $\frac{1}{D(f^{(1)}_{(m,n)} \parallel f_0)}$ for large mean time to false alarm [21].

From the plots, we conclude that for the same value of mean time to false alarm, both CuSum-based algorithms have a much lower average detection delay compared to the Shewhart and meanshift algorithms. In addition,

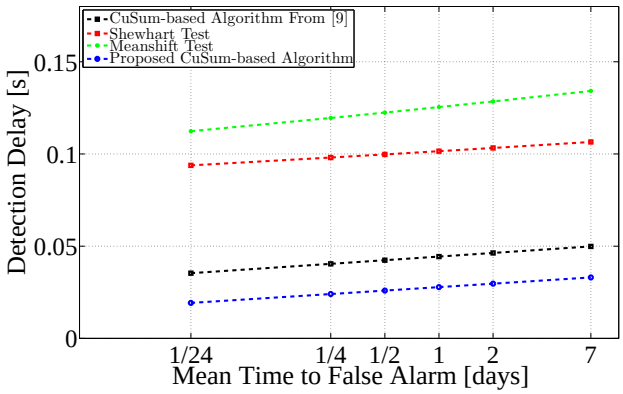

Figure 3.4: Detection delay vs. mean time to false alarm.

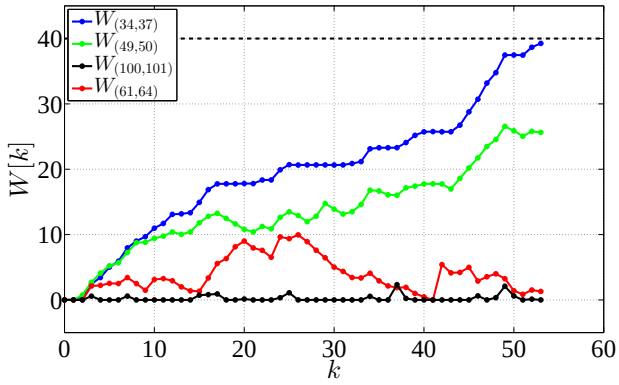

Figure 3.5: Sample run of 118-bus system.

the figure shows that when we use varied thresholds for the CuSum test as opposed to a fixed threshold, even lower detection delay can be achieved for the same mean time to false alarm. This illustrates that our algorithm is an improvement over that of [13]. Lastly, simulation results demonstrate that the detection delay scales exponentially with the selected thresholds for both the meanshift and Shewhart tests, and linearly for the CuSum-based tests.

3.6.3 118-Bus System

Next, we illustrate the scalability of the proposed line outage detection algorithm on the IEEE 118-bus test system. The simulation tool MATPOWER [32] is used to compute the voltage angles by repeatedly solving AC power flow solutions of the system. The real power injection is generated using (3.13) with $\sigma = 0.03$. We also assume these random fluctuations are uncorrelated; thus, Λ is a diagonal matrix.

An outage in line $(34, 37)$ starting at $k = 1$ is simulated and the algorithm of (3.2) is applied. Some sample test statistics are shown in Fig. 3.5. With a threshold of 40, the line outage is declared 53 samples after the outage.

3.7 Summary

In this chapter, the CuSum algorithm for change detection was introduced along with the GLRT algorithm, which serves as a basis for the line-outage detection method proposed in this thesis. We also introduced other line out-

age detection algorithms in literature and compare their performance against our proposed method. We showed that the CuSum algorithm performs better since it uses the statistical properties of the measured voltage phase angles before, during, and after a line outage, whereas other methods in the literature only utilize the change in statistics that occurs at the instant of outage.

CHAPTER 4

LINE OUTAGE DETECTION CONSIDERING TRANSIENTS

This chapter improves the line outage detection algorithm presented in Chapter 3 by taking into account the transient dynamics that the system experiences immediately after the outage occurrence. More specifically, the generators respond to the power mismatch according to the so-called "governor power flow model". Hence we incorporate this phenomenon into our detection scheme for better performance. The notion of ranked list is also introduced for capturing the probability of false isolation.

4.1 Generalized CuSum Test

Recall the statistical model in (2.16):

$$\Delta\hat{\theta}[k] \sim \begin{cases} f_0 \coloneqq \mathcal{N}(0, \hat{M}_0 \Lambda \hat{M}_0^T), \text{ if } 1 \leq k < \gamma_0, \\ f_{(m,n)}^{(0)} \coloneqq \mathcal{N}(-P_{(m,n)}[\gamma_0 + 1] C M_0 r_{(m,n)}, \\ \qquad\qquad \hat{M}_0 \Lambda \hat{M}_0^T), \text{ if } k = \gamma_0, \\ \vdots \\ f_{(m,n)}^{(T)} \coloneqq \mathcal{N}(0, \hat{M}_{(m,n),T} \Lambda \hat{M}_{(m,n),T}^T), \text{ if } k \geq \gamma_T. \end{cases} \tag{4.1}$$

The Generalized CuSum (G-CuSum) discussed in Chapter 3 was developed with the understanding that the transition between pre- and post-outage periods is not characterized by any transient behavior other than the meanshift that occurs at the instant of outage (e.g., $T = 1$). The meanshift was captured by introducing an additional log-likelihood ratio term between the distribution at the time of change and the distribution before the change. The final test statistic takes the maximum of this log-likelihood ratio and the traditional G-CuSum test recursion.

Although the G-CuSum algorithm does not take any transient dynamics into consideration, it can still perform well when the transient distributions

and the final post-change distribution are "similar", i.e., when the KL divergence between $f^{(i)}_{(m,n)}$, $i = 1, 2, \ldots, T-1$, and $f^{(T)}_{(m,n)}$ is small. As a result, it is useful to compare the performance of the G-CuSum test with the performance of the G-D-CuSum test that is proposed in this work.

Since the line that is outaged is not known a priori, the G-CuSum test works by using the CuSum test statistics in a generalized manner. As a result, we compute L CuSum statistics in parallel, one corresponding to each line outage scenario, and declare a change when an outage to any line is detected. The CuSum recursion for line (m, n) is calculated by accumulating log-likelihood ratios between $f^{(T)}_{(m,n)}$ and f_0.

4.2 Generalized Dynamic CuSum Test

Since the proposed statistical model in (2.16) can include an arbitrary number of transient periods with finite duration, each one corresponding to a respective transient distribution induced on the observations, it is clear that the G-CuSum test of [33] needs to be modified to take this transient behavior into consideration. Toward this end, we introduce the Generalized Dynamic CuSum (G-D-CuSum) test. This test is derived by exploiting the so-called Dynamic CuSum (D-CuSum), a test also proposed in this work. This test arises as a solution to the non-composite QCD problem under the presence of an arbitrary number of transient periods. The D-CuSum test statistic is derived by formulating the transient QCD problem as a dynamic composite hypothesis testing problem at each time instant. The G-D-CuSum algorithm uses the test statistics of the D-CuSum test in a generalized manner, i.e., calculates a test statistic for each possible line outage in parallel, and declares an outage when one of the line statistics crosses a pre-determined positive threshold corresponding to the line.

By using the D-CuSum test statistic as a basis, we propose the G-D-CuSum test. The statistic for line (m, n) is given as follows:

$$W^{\mathrm{D}}_{(m,n)}[k] = \max\left\{\Omega^{(1)}_{(m,n)}[k], \ldots, \Omega^{(T)}_{(m,n)}[k], \log\frac{f^{(0)}_{(m,n)}(\Delta\hat{\theta}[k])}{f_0(\Delta\hat{\theta}[k])}\right\}, \tag{4.2}$$

where

$$\Omega^{(i)}_{(m,n)}[k] = \max\left\{\left[\max\{\Omega^{(i)}_{(m,n)}[k-1], \Omega^{(i-1)}_{\ell}[k-1]\} + \log\frac{f^{(i)}_{(m,n)}(\Delta\hat{\theta}[k])}{f_0(\Delta\hat{\theta}[k])}\right], 0\right\}, \tag{4.3}$$

for $i \in \{1, \ldots, T\}$, $\Omega^{(0)}_{(m,n)}[k] \coloneqq 0$ for all $k \in \mathbb{Z}$ and $\Omega^{(i)}_{(m,n)}[0] \coloneqq 0$ for all $(m,n) \in \mathcal{E}$ and all i. The corresponding stopping rule is defined as

$$\tau^{\mathrm{D}} = \inf_{(m,n)\in\mathcal{E}}\left\{\inf\{k \geq 1 : W^{\mathrm{D}}_{(m,n)}[k] > A_{(m,n)}\}\right\}. \tag{4.4}$$

Calculating the test statistic for line (m,n) involves calculating the statistics $\Omega^{(1)}_{(m,n)}, \ldots, \Omega^{(T)}_{(m,n)}$. The final test statistic is given by taking the maximum of these terms together with the log-likelihood ratio between the distribution at the outage and the pre-outage distribution. Note that to renew each Ω statistic, the value of the statistic in the previous time instant and the value of the statistic used to detect the previous distribution change is used. The basis of this algorithm is that each statistic is used to capture one of the transient distributions. As a result, at each different period that the process goes through, one of the Ω statistics will dominate the others, leading to the adaptive nature of the algorithm. Also, the test statistics are designed to use prior information from other test statistics, exploiting the fact that distribution changes occur in a sequential manner. A detailed derivation of this algorithm is presented in Appendix B.

4.3 Line Outage Identification

The detection algorithm proposed in Chapter 3 can also be used to identify the outaged line. One strategy would be to declare the outaged line as the one corresponding to the largest statistic at the stopping time. To this end, denote by $\hat{l}$ the line that is identified as outaged. Then,

$$\hat{l} = \arg\max_{(m,n)\in\mathcal{E}} W_{(m,n)}[\tau]. \tag{4.5}$$

A drawback of this line outage identification method is that the statistics for other lines may also increase following a line outage. Due to the structure of a power system, certain line outages may result in multiple line statistics, in addition to the one corresponding to the true outaged line, to increase. Therefore, in order to reduce the probability of false isolation, a *set* of lines is identified as potentially outaged. Consequently, more than one line should be checked by the system operator after an outage is declared. We associate with each line statistic a corresponding ranked list. The idea is similar to listed decoding in digital communications (see e.g., [34]).

This ranked list contains line indices for which the line statistics grow almost as fast as the true outaged line. The ranked list can be created offline by computing the growth rate of each statistic for each line outage in advance, either through a full simulation of the power system, or theoretically, by inspecting the post-outage KL divergences. Since there are multiple transient periods following a line outage, it is important to use the correct post-outage distribution in the calculation of the KL divergence. Intuitively, for a specific threshold choice and line outage, knowledge of the average delay provides information regarding the post-outage period during which the outage is declared. It is natural to believe that the KL divergence between the distribution corresponding to this stage and the pre-outage distribution plays the major role in the behavior of the test statistic; thus it should be used to create the ranked list for the examined line.

Define the ranked list for statistic $W_{(m,n)}$ as

$$\mathcal{C}_{(m,n)} = \{(m,n)_1, \ldots, (m,n)_{C_{(m,n)}}\}, \tag{4.6}$$

where $C_{(m,n)}$ the cardinality of the ranked lists and $(m,n) \in \mathcal{C}_{(m,n)}$.

To quantify the performance of our algorithm with respect to its ability to identify the outaged line accurately, we define the probability of false isolation (PFI). For the case of line (m,n) outage, a false isolation event occurs when (m,n) is not included in the ranked list of the line statistic with the highest value at the time of stop. Define the PFI when line (m,n) is outaged as:

$$\mathrm{PFI}_{(m,n)}(\tau) = \mathbb{P}\{(m,n) \notin \mathcal{C}_{\hat{l}} | \text{line } (m,n) \text{ outage}\}. \tag{4.7}$$

The length of ranked lists should be chosen to optimize the tradeoff between

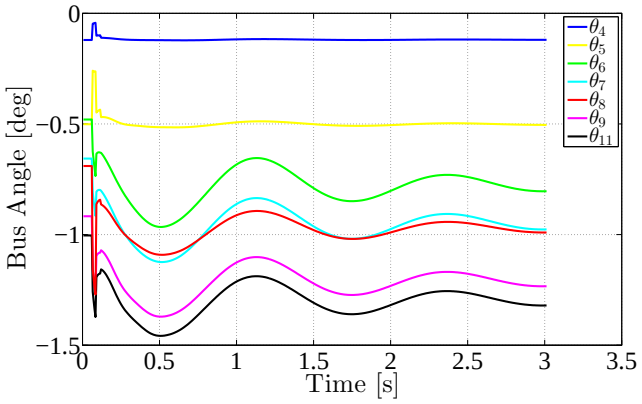

Figure 4.1: Voltage phase angles of IEEE 14-bus system following an outage in line 7.

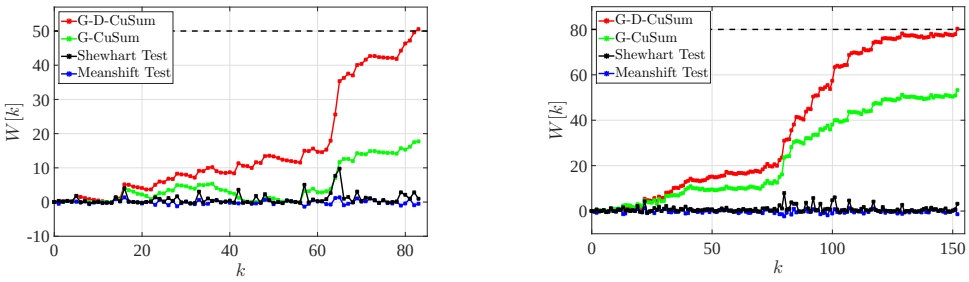

(a) Line 9 outage with A_l=50.

(b) Line 9 outage with A_l=80.

Figure 4.2: Sample paths for IEEE 14-bus system.

PFI and number of lines that need to be checked after an outage detection has occurred. In particular, larger ranked lists lead to lower PFI, but to a larger set of possibly outaged lines. Detailed simulation results for the PFI values of our proposed algorithm are presented in Section 5.4.

4.4 Case Studies

In this section, the algorithm proposed in (4.2)-(4.4) is applied to the IEEE 14-bus, and the IEEE 118-bus test systems (for the model data, see [31]). In order to compute the transient dynamics following a line outage, we use the simulation tool Power System Toolbox [35]. For simplicity, we used the statistical model in (2.16) with $T = 2$, i.e., we assumed one transient period after the line outage occurs. Additional transient periods could easily be incorporated into the simulations. The power injection profiles at the load buses are assumed to be independent Gaussian random variables with vari-

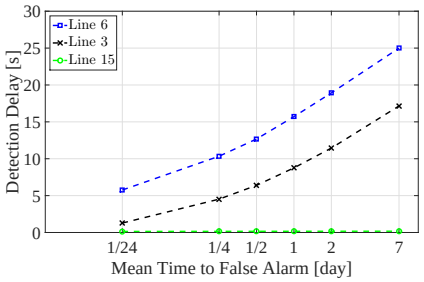

(a) Detection delay vs. mean time to false alarm for different lines.

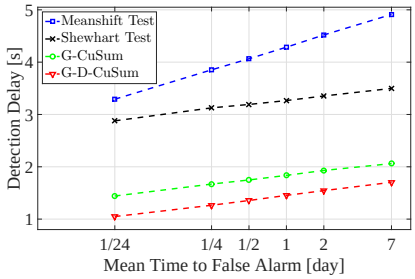

(b) Detection delay vs. mean time to false alarm for different algorithms.

Figure 4.3: IEEE 14-bus Monte Carlo simulation results.

ance of 0.03 and the PMU sampling rate is assumed to be 30 measurements per second. For our simulations, we found that the error bounds for all the simulated values are within 5% of the means.

4.4.1 14-bus System

For the IEEE 14-bus system, we simulated an outage in line 7 at $t = 0.1$s. The dynamic responses of the voltage phase angles are shown in Fig. 4.1. From the plots, we conclude that the transient period following a line outage lasts approximately 3 seconds, which is assumed in the model for our proposed detection algorithm.

Next, we simulate two different line outages for the 14-bus test system, one in which the detection occurs during the transient period and one in which the detection occurs after the transient period; the results are shown in Fig. 4.2. Figure 4.2(a) shows some typical progressions of $W_9[k]$'s for the various line outage detection schemes discussed earlier. The fault occurs at $k = 10$ and the threshold is $A_{(m,n)} = 50$. The transient period was assumed to last for 100 samples (approximately 3 seconds). From the figure, we conclude that for this sample run, a line outage is declared after 74 samples when the G-D-CuSum stream crosses the threshold first. The other algorithms incur a much larger detection delay since they do not cross the threshold of $A_{(m,n)} = 50$. Figure 4.2(b) shows the typical progressions of $W_9[k]$'s for an outage in line 9. For a threshold of $A_{(m,n)} = 80$, the G-D-CuSum detects a line outage 138 samples after the outage occurs. In this example, the detection occurs after the transient dynamics have subsided. From the plots, we conclude

Table 4.1: False isolation probability obtained via simulation for IEEE 14-bus system.

$\mathbb{E}_0[\tau]$ [day]	1/24	1/4	1/2	1	2	7
Line 3	0.0312	0.0255	0.0230	0.0214	0.0209	0.0197
Line 6	0.0139	0.0094	0.0059	0.0044	0.0031	0.0022
Line 15	0.0112	0.0079	0.0052	0.0044	0.0030	0.0021

that even though detection takes place after the transient dynamics subside ($k = 110$), the G-D-CuSum algorithm still has a smaller detection delay than the G-CuSum algorithm.

We performed Monte Carlo simulations for outages in lines 3, 6, and 15, and show the detection delay versus mean time to false alarm in Fig. 4.3(a). Among all the lines of the system, detection delay for line 15 is the lowest for a fixed mean time to false alarm while line 6 has the worst detection delay. Line 3 was chosen as a representative line for intermediate delay values. Inspecting 4.3(a), we come to the conclusion that detection of line 3 and line 6 outage is happening after the transient period is over for the majority of the sample runs. This is also reflected on the slope change of these two lines. In particular, after the transient dynamics subside, the slope of the delay lines gradually changes, since the dominant KL divergence is that between the persistent post-outage distribution and the pre-outage distribution. Additionally, we compared the performance of our proposed algorithm against the Meanshift test, Shewhart test, and the G-CuSum algorithm for an outage on line 7, and the results are shown in Fig. 4.3(b). From the plot, we conclude that the G-D-CuSum algorithm achieves the lowest detection delays among all algorithms for a given mean time to false alarm.

Finally, the PFI versus mean time to false alarm is obtained for outages in lines 3, 6, and 15; the results are recorded in Tab. 4.1. The PFI was calculated by using the clustering technique discussed in Section 4.3. The ranked list for the 14-bus system line statistics is shown in Tab. 4.2. A maximum number of three lines per ranked list was used. Table 4.2 indicates, for each statistic, the set of 3 lines that are most likely to have contributed to this line statistic achieving large values. For example, a large value of statistic W_2^{D} is most likely caused by an outage in line 2, 4, or 5. Note

that the PFI decreases as the mean time to false alarm increases. This is because larger mean time to false alarm corresponds to larger thresholds, which result in smaller PFI values. Finally, line 14 do not have a ranked list since its outage causes the system to island into two smaller subsystems.

4.4.2 118-bus System

To illustrate the scalability of the proposed algorithm, we simulate outages in lines 60, 180, and 186. The detection delay versus false alarm for these lines is shown in Fig. 4.4. From the plots, we conclude that among the three lines, line 186 has the best line outage detection performance. That is, for a fixed mean time to false alarm, a line 186 outage has the lowest detection delay. Meanwhile, line 60 has the worst detection performance and line 180 is in the middle. Finally we estimated the PFI for different mean times to false alarm through Monte Carlo simulations. We use the same clustering technique as for the 14-bus system with a maximum of three lines per ranked list on the 118-bus system. However, due to space constraints, we omit the ranked list table for the 118-bus system. The PFI results for lines 60 and 180 are shown in Tab. 4.3. The PFI results for line 186 outage are not shown because after extensive simulations, we found the values to be all smaller than 10^{-7}. The PFI values are similar to the 14-bus system with PFI decreasing as the mean time to false alarm increases.

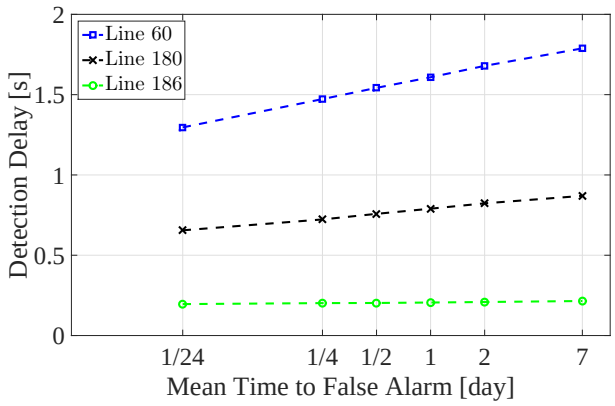

Figure 4.4: 118-bus: Detection delay versus mean time to false alarm for different lines for the IEEE 118-bus system.

Table 4.2: 14-bus system: Ranked list

Statistics	W_1^D	W_2^D	W_3^D	W_4^D	W_5^D
Lines	$\{1, 2, 4\}$	$\{2, 4, 5\}$	$\{3, 4, 6\}$	$\{2, 3, 4\}$	$\{3, 5, 6\}$
Statistics	W_6^D	W_7^D	W_8^D	W_9^D	W_{10}^D
Lines	$\{3, 5, 6\}$	$\{1, 2, 7\}$	$\{1, 7, 8\}$	$\{2, 4, 9\}$	$\{1, 10, 17\}$
Statistics	W_{11}^D	W_{12}^D	W_{13}^D	W_{14}^D	W_{15}^D
Lines	$\{1, 10, 17\}$	$\{1, 11, 13\}$	$\{1, 12, 19\}$	$\emptyset$	$\{1, 8, 15\}$
Statistics	W_{16}^D	W_{17}^D	W_{18}^D	W_{19}^D	W_{20}^D
Lines	$\{1, 15, 16\}$	$\{1, 17, 20\}$	$\{1, 11, 18\}$	$\{1, 12, 19\}$	$\{1, 17, 20\}$

Table 4.3: False isolation probability obtained via simulation for IEEE 118-bus system.

$\mathbb{E}_0[\tau]$ [day]	1/24	1/4	1/2	1	2	7
Line 60	0.0295	0.0183	0.0176	0.0127	0.0103	0.0087
Line 180	0.0237	0.0132	0.0101	0.0087	0.0059	0.0031

4.5 Summary

In this chapter, we proposed a modified line outage detection algorithm that performs better than previous methods of line outage detection because it is adaptable to the transient dynamics that occur in the system following a line outage. This algorithm features a set of statistics which are used to capture each distribution shift. The algorithm is derived as a generalization of the generalized likelihood ratio solution of the transient QCD problem. The detection delay performance of the proposed algorithm is compared against other line outage detection algorithms for line outages simulated on the IEEE 14- and 118-bus test systems.

CHAPTER 5

OPTIMAL PMU PLACEMENT AND SYSTEM PARTITIONING

In this chapter we present several extensions of the quickest change detection algorithm presented in Chapter 3. A method to choose the threshold for each CuSum statistic resulting in better performance is proposed. We also formulate the optimal PMU placement strategy for the given power system network so that the worst case detection delay is minimized. Additionally, we show that our method could be applied to each area of a partitioned power system concurrently for faster detection, and provide several criteria to obtain such partitions.

5.1 PMU Placement

It turns out that the definition of KL divergence presented in equation (3.11) has a closed form solution if the two distributions f and g are Gaussian. Since the pre-outage distribution, $f_0 = \mathcal{N}(0, \hat{M}_0 \Sigma \hat{M}_0^T)$, and the post-outage distribution, $f_{(m,n)} = \mathcal{N}(0, \hat{M}_{(m,n)} \Sigma \hat{M}_{(m,n)}^T)$, are both Gaussian, we can express $D(f_{(m,n)} \parallel f_0)$ as (for derivation, see Appendix A.2)

$$\frac{1}{2}\big[\mathrm{Tr}(\Gamma_0^{-1}\Gamma_{(m,n)}) - p + \log(\det(\Gamma_0 \Gamma_{(m,n)}^{-1}))\big], \tag{5.1}$$

where $p \leq N^d$ is the number of PMUs allocated for the system, $\Gamma_0 = \hat{M}_0 \Sigma \hat{M}_0^T$, and $\Gamma_{(m,n)} = \hat{M}_{(m,n)} \Sigma \hat{M}_{(m,n)}^T$.

From equation (5.1), it is evident that the KL divergences depend on p, the number of PMUs allocated for the system. In addition, for a fixed p, the locations of the PMUs also affect the KL divergences. In order to minimize the worst case detection delay for all line outages, the following optimization can be solved for the optimal placement of the p PMUs:

$$\max_{C} \min_{\Gamma_{(m,n)}} \frac{1}{2}\big[\mathrm{Tr}(\Gamma_0^{-1}\Gamma_{(m,n)}) - p + \log(\det(\Gamma_0\Gamma_{(m,n)}^{-1}))\big]. \tag{5.2}$$

The inner minimization is over all possible line outages in the system since we would like to minimize the detection delay for the worst possible line outage case. Some techniques for solving this optimization include cutting-plane method and branch and bound method [36].

The integer programming problem in (5.2) is NP hard; therefore, in order to speed up the combinatorial search, we propose a greedy algorithm, the pseudocode of which is provided in Algorithm 1; this algorithm provides a lower bound to the globally optimal solution. The algorithm chooses the locations of the PMUs sequentially. At each step, we select the additional location of the PMU to be the one that maximizes the current minimum KL divergence for all possible line outages and add it to the current PMU selection. The algorithm stops when the number of PMUs selected reaches p. We show in the case studies that this method is computationally tractable with good performance.

Algorithm 1: Greedy Algorithm for PMU placement

```
Data: N, p
C = 0, k = 0;
for k = 1 to p do
    g = 0;
    for n = 1 to N do
        C(k,:) = e_n^T;
        KL = min_{Γ_i}  (1/2)[Tr(Γ_0^{-1}Γ_i) − p + log(det(Γ_0Γ_i^{-1}))];
        if g < KL then
            g = KL;
            l = n;
        end
    end
    C(k,:) = e_l^T;
end
return C
```

***Example* 5.1** (Three-Bus System with Limited PMUs)**.** Now consider the same 3-bus system as in Example 3.1 but with PMU deployed at only bus 2 instead of both buses 2 and 3. The typical progressions of $W_{(m,n)}[k]$ for each line outage of the 3-bus system are simulated and plotted in Fig. 5.1.

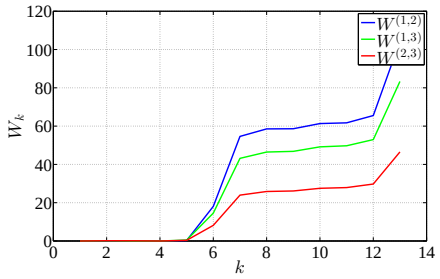

(a) Line $(1, 2)$ outage.

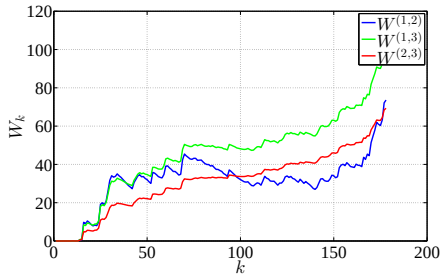

(b) Line $(1, 3)$ outage.

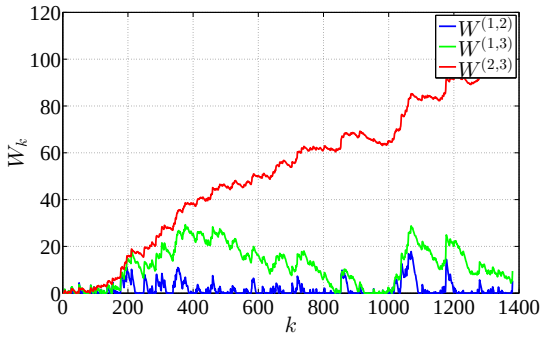

(c) Line $(2, 3)$ outage.

Figure 5.1: Realizations of $W_{(m,n)}[k]$ for each line outage of 3-bus system with PMU at bus 2 only.

Table 5.1 shows the computed KL divergences for this example. With the removal of one PMU from this system, the KL divergences for all line outages decreased. This is also evident from the plots, where on average, the $W_{(m,n)}[k]$'s now required more samples to reach the same threshold A, resulting in longer detection delays. □

***Example* 5.2** (14-Bus System PMU Placement)**.** Consider the IEEE 14-bus test system, the one-line diagram of which is shown in Fig. 3.2. The PMU measurements for the voltage phase angles are simulated by creating an active power injection time-series data set and using it to compute the voltage phase angles via the nonlinear power flow model. The power injection for each load bus i is simulated by

$$P_i^d[k] = P_i^d[k-1] + v_i, \tag{5.3}$$

where $P_i^d[0]$ is the nominal power demand at bus i and $v_i \sim \mathcal{N}(0, 0.3)$ is a pseudorandom value representing random fluctuations in electricity consumption. In addition, we assume that the random fluctuations at all the

Table 5.1: 3-bus system KL Div. with PMU at bus 2.

KL Div. \ Line Outage (m,n)	$(1,2)$	$(1,3)$	$(2,3)$
$\mathbb{E}\left[\log\left(\frac{f_{(1,2)}}{f_0}\right) \mid (m,n) \text{ outage}\right]$	2.9	0.33	-0.38
$\mathbb{E}\left[\log\left(\frac{f_{(1,3)}}{f_0}\right) \mid (m,n) \text{ outage}\right]$	2.51	0.52	-0.03
$\mathbb{E}\left[\log\left(\frac{f_{(2,3)}}{f_0}\right) \mid (m,n) \text{ outage}\right]$	1.46	0.37	0.06

load buses are independent, so Λ is a diagonal matrix.

An outage in line $(2,5)$ is simulated at $k = 10$. We apply the Generalized CuSum algorithm in (3.2) by computing $W_{(m,n)}[k]$ for each line of the system. A uniform threshold of $A = 100$ is used for all CuSum statistics, $W_{(m,n)}[k]$. Figure 5.2 shows the typical progressions of $W_{(m,n)}[k]$ for an outage in line $(2,5)$. Figure 5.2(a) assumes a full measurement set of voltage phase angles, while Fig. 5.2(b) is simulated with a reduced measurement set, where PMUs are deployed randomly at only nine of the buses. In both cases, the line outage is correctly identified when the $W_{(2,5)}$ statistic crosses the threshold of $A = 100$ first. With a full measurement set, the correct line outage is identified 65 samples after the outage occurs while a much longer detection delay of 170 samples is needed for the reduced measurement set.

Now suppose that we select nine buses via the procedure in Algorithm 1. The typical progressions of $W_{(m,n)}[k]$ for this case are shown in Fig. 5.2(c). By optimally placing the PMUs, we have reduced the detection delay to 79 samples, which is significantly better than randomly choosing the nine PMU locations. □

5.2 Power System Network Partitioning

For scalability, the graph describing the topology of a power system could be partitioned into subgraphs and the quickest change detection algorithm could be applied to each partition in parallel. This would allow for easier implementation of double line outage detection and scaling to larger systems but would require novel approaches to solving the current line outage detection problem. There are many ways we can partition the overall system according to some optimality criteria; we consider three possible criteria here:

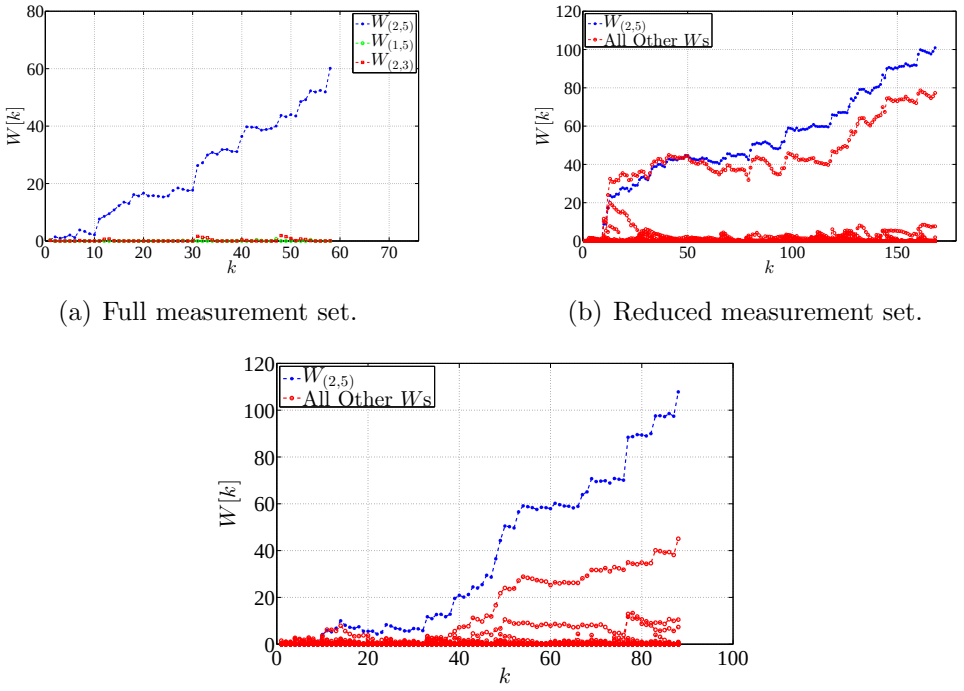

(a) Full measurement set.

(b) Reduced measurement set.

(c) Optimal reduced measurement set.

Figure 5.2: 14-bus system: Sample paths of $W_{(m,n)}[k]$ for outage of (2,5).

C1. Equal number of edges within each partition (balanced size for each partition).

C2. A partition such that the number of detectable single-line outage for the overall system is maximized.

C3. Minimum KL divergence for all the partitions is maximized (to minimize detection delay).

[C1.] Suppose each processor carrying out the line-outage detection algorithm could perform computations on K streams of data in parallel and there are L total lines in the overall system. Then the ideal number of partitions for the system such that all processors are fully utilized is $\lceil \frac{L}{K} \rceil$. One particular graph partitioning algorithm minimizes the number of edges (or the sum of their associated costs) in the cut-set of the graph while constraining the upper bound on the number of nodes in each partition [37]. This algorithm is based on computing the spectral factorization of the partition matrix. Another graph partitioning software is the METIS package [38]. It is a k-way partitioning method based the Kernighan-Lin algorithm with multilevel

Table 5.2: 14-bus min. KL Div.

no. PMUs	1	2	3	4	5	6	7	8	9	10	11	12
Optimal	0.029	0.045	0.094	0.37	0.40	0.54	0.60	0.62	0.62	0.64	0.64	0.64
Greedy	0.027	0.043	0.056	0.19	0.22	0.23	0.25	0.37	0.49	0.61	0.64	0.64

graph coarsening. This software partitions a graph into k partitions based on two possible objective functions, minimum edgecut or minimum communication volume (based on weights assigned to border vertices). Hence, one form of quasi-optimality for partitioning is to balance the number of edges *within* each partition; once the number of edges within each partition is specified, then the problem becomes finding the set of partitions such that the minimum KL divergence in each partition is maximized. It is worth mentioning that the number of edges in the cutset should be minimized since outages for these lines are unobservable through the QCD algorithm. The problem of balancing edges in every partition may be transformed into a problem of balancing the in/out degrees of the vertices in a partition.

[C2.] If the removal of an edge in the partition further divides the graph into subgraphs (this corresponds to islanding in the power system partition), then such a line outage is undetectable by the QCD method. A good partitioning scheme maximizes the number of detectable single-line outages for the overall system.

[C3.] The optimal partition should minimize the false alarm and false isolation rate. The false isolation rate decays exponentially with the threshold A while the average detection delay is inversely proportional to the KL divergence. The problem of finding the optimal partitioning of the system would then be formulated as

$$\max_{\text{all partitions}} \min_{\Gamma_{(m,n)}} \frac{1}{2}\big[\mathrm{Tr}(\Gamma_0^{-1}\Gamma_{(m,n)}) - p + \log(\det(\Gamma_0\Gamma_{(m,n)}^{-1}))\big]. \tag{5.4}$$

Constraints can be added to the optimization problem as necessary. These constraints include the maximum number of edges in each partition, the maximum number of vertices in each partition, or the number of partitions for the overall system.

***Example* 5.3** (14-Bus System Partitioning)**.** We adopt Criterion **C1** and use the METIS software package to partition the network of the IEEE 14-bus system utilized in Example 5.2. For a partition size of 2, this program separates the 14-bus system into areas with approximately equal number of

nodes while minimizing the number of tie-lines between the two areas. The result from the graph partitioning algorithm is as follows:

- Area 1: Buses 1, 2, 3, 4, 5, 7, 8
- Area 2: Buses 6, 9, 10, 11, 12, 13, 14.

For a partition size of 2, this algorithm separated the 14-bus system into areas with approximately equal number of nodes while minimizing the number of tie-lines between the two areas. While such a partition choice is favorable from the perspective of requiring the least number of direct line power flow measurements for the tie lines, it does not minimize the total number of unobservable line outages for the overall system. This is evidenced by the fact that an outage on lines $(10, 11)$ or $(13, 14)$ causes islands to form in Area 2.

Next, we compute the minimum KL divergences for the entire 14-bus system, Area 1, and Area 2 of the partitioned 14-bus system to compare how they are affected by the number of PMUs deployed. Figure 5.3 shows how the minimum KL divergence increases as more PMUs are added, using both an exhaustive search that is globally optimal and the greedy Algorithm 1. The results for the entire 14-bus system are shown in Fig. 5.3(a) while those for Area 1 and Area 2 of the partitioned 14-bus system are shown in Fig. 5.3(b) and Fig. 5.3(c), respectively. The values of the KL divergence as more PMUs are added for the entire 14-bus system are also listed in Tab. 5.2. From the plots, we conclude that the greedy algorithm provides a lower bound to the exhaustive search because the greedy algorithm is only traversing one of the many branches of the branch and bound method. Although not globally optimal, the greedy algorithm is attractive in the sense that is it tractable for larger systems. □

5.3 On Selection of Threshold

In [13], a single threshold A was chosen for all line outage streams $W[k]$. However, we show that faster detection can be achieved by choosing a threshold $A_{(m,n)}$ for $W_{(m,n)}[k]$ that is scaled by its respective KL divergence:

$$A_{(m,n)} = \alpha \frac{D(f_{(m,n)}||f_0)}{\max\limits_{(k,l)\in\mathcal{E}} D(f_{(k,l)}||f_0)}, \tag{5.5}$$

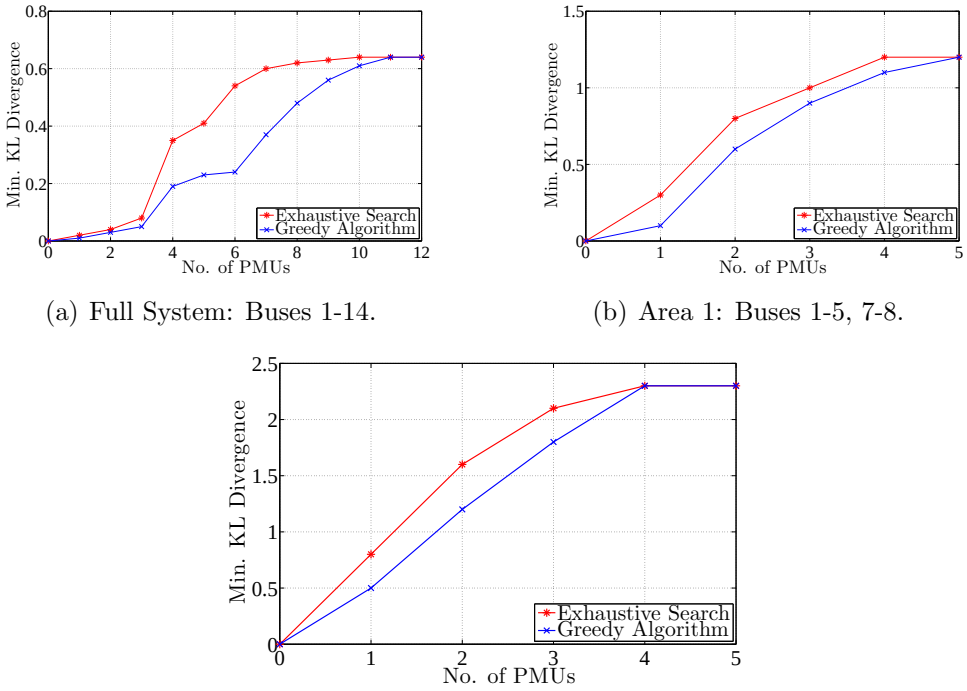

(a) Full System: Buses 1-14.

(b) Area 1: Buses 1-5, 7-8.

(c) Area 2: Buses 6, 9-14.

Figure 5.3: Minimum KL divergence of 14-bus system.

where α is a positive scaling constant and D is the KL divergence defined next. We illustrate this idea of scaling $A_{(m,n)}$ individually with α in Section 5.4 with case studies on the IEEE 118-bus system. The threshold $A_{(m,n)}$ can also be chosen to control the mean time to false alarm; if a larger mean time to false alarm is required, then $A_{(m,n)}$ is set to a larger value, and vice-versa.

5.4 Case Studies

In this section, we illustrate the ideas proposed in this paper on the IEEE 30-bus and the IEEE 118-bus test systems. The one-line diagrams for these systems can be found in [31].

5.4.1 30-bus System

For the IEEE 30-bus system, we partition the system into two areas using the METIS software and compute the minimum KL divergence in Area 2 (buses 10, $12-30$) to see how it is affected by the number of PMUs deployed

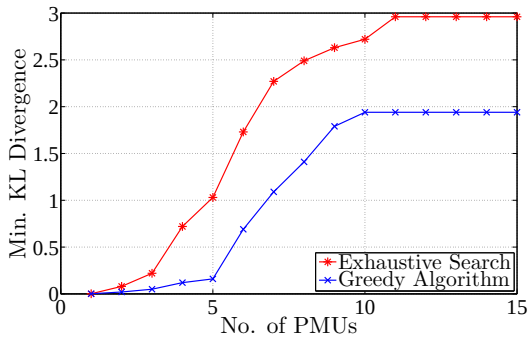

Figure 5.4: Minimum KL Div. of Area 2 of 30-bus system.

throughout the partition. We apply both the greedy algorithm (the pseudocode of which is provided in Algorithm 1) and an exhaustive search and show the results in Table 5.3 and Fig. 5.4. Using MATLAB running on an Intel Core i7 Processor, the greedy algorithm required less than 2 minutes to run, while 3 days were required for the optimal PMU placement via exhaustive search. For the exhaustive search method, the number of computations required for each partition is $\binom{N_i}{p}$ while the greedy algorithm requires only $N_i p$ computations, where N_i is the number of buses in partition i.

Next we simulate a line outage on line $(15, 23)$ of Area 2, which has a KL divergence of 14.3. The threshold is set at $A = 200$ with the variance of active power injections assumed to be 0.3 at all of the load buses. Typical progressions of $W_{(m,n)}[k]$ are shown in Fig. 5.5. For this particular example, $W_{(15,23)}$ crosses the threshold of $A = 200$ for the first time 23 samples after the outage occurs, resulting in a detection delay of 0.76 seconds.

Finally, we compare how the average detection delay of *all* possible line outages is related to the detection threshold. For a particular chosen thresh-

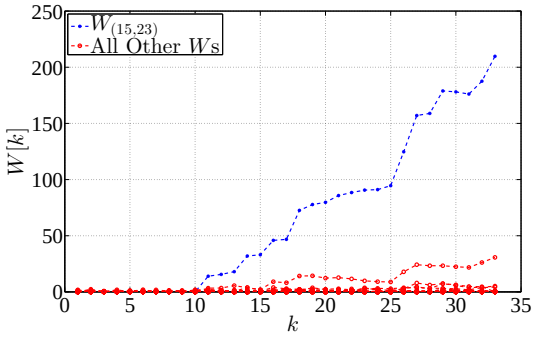

Figure 5.5: 30-bus system: Sample paths of $W_{(m,n)}[k]$ for line outage of (15,23) of Area 2.

Table 5.3: 30-bus system: Minimum KL divergence of Area 2.

no. PMUs	1	2	3	4	5	6	7
Optimal	0.0012	0.08	0.22	0.72	1.03	1.73	2.27
Greedy	0.0012	0.02	0.05	0.12	0.16	0.69	1.09
no. PMUs	8	9	10	11	12	13	14
Optimal	2.49	2.63	2.72	2.96	2.96	2.96	2.96
Greedy	1.41	1.79	1.94	1.94	1.94	1.94	1.94

Table 5.4: 30-bus system: α vs. Average Detection Delay of all lines.

α	10	20	30	40	50	60	70	80	90	100
Avg. Detection Delay [s]	0.25	0.49	0.73	0.99	1.23	1.47	1.84	1.93	2.20	2.46
Uniform A	10	20	30	40	50	60	70	80	90	100
Avg. Detection Delay [s]	2.02	4.04	6.07	8.09	10.13	12.06	14.18	16.23	18.19	20.21

old $A_{(m,n)}$, we perform Monte Carlo simulations to obtain the average detection delay for the outage in line (m, n). Then, we compute the mean of the average detection delay of all lines in the power system. The top half of Table 5.4 shows the mean of the average detection delay of all lines resulting from selecting the thresholds $A_{(m,n)}$ through α and scaled according to (5.5). The bottom half of Table 5.4 shows the results due to selecting a threshold uniformly across all lines. From the results, we observe that scaling the thresholds according to KL divergences incurs a much lower mean average detection delay. In addition, we note that for either method of selecting the threshold, the detection delay scales linearly with the threshold.

5.4.2 118-bus System

Next for the IEEE 118-bus system, we simulate an outage in line $(60, 62)$ at $k = 1$. Figure 5.6 shows two realizations of $W[k]$ for the same outage. In Fig. 5.6(a), the detection threshold was set at $A = 100$ for all $W[k]$s. In Fig. 5.6(b), the threshold for each $W[k]$ was scaled linearly to the KL divergence according to (5.5) with $\alpha = 100$. Comparing the two cases, we conclude that by choosing the thresholds scaled appropriately according to the KL divergences, much lower detection delay can be achieved. This was also verified through extensive Monte Carlo simulations where a threshold of $A = 100$ resulted in an average detection delay of 42 samples, whereas scaling the threshold reduced the average detection delay to 21 samples.

Next, we compare the average detection delay versus mean time to false

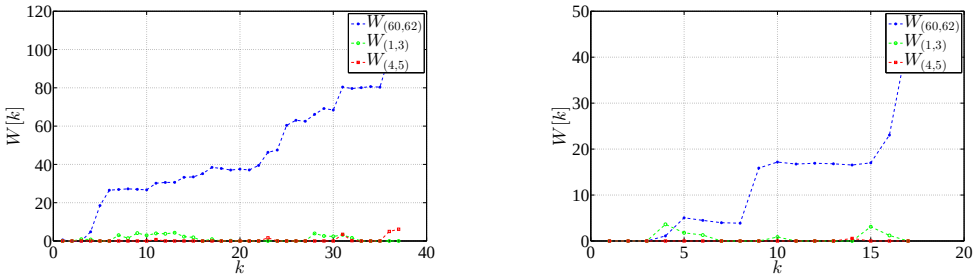

(a) Uniform threshold. (b) Scaled thresholds.

Figure 5.6: 118-bus system: Sample paths of $W_{(m,n)}[k]$ for outage of (60, 62).

alarm of our proposed CuSum line outage detection method. We perform $50,000$ sample runs of outages on lines $(60, 62)$ and $(62, 66)$ to compute the average detection delay and then another $50,000$ sample runs for the false alarm data. The results are shown in Fig. 5.7 with the PMU sampling rate assumed to be 30 samples per second. We conclude that even for large mean time to false alarm, the detection delays are quite low for the line outages studied.

Finally, we apply Algorithm 1 for deploying PMUs across the 118-bus system. For each configuration of PMUs, we simulate the average detection delay of all line outages with a uniform threshold of $A = 100$ for all $W[k]$s. The results are shown in Fig. 5.8. From the figure, it is evident that the first several PMUs have the most impact in reducing detection delay. As the number of PMUs increases, the marginal benefit decreases. It was also observed that in general having PMUs at one-third of the buses is sufficient to achieve average detection delays that are close to the globally optimal

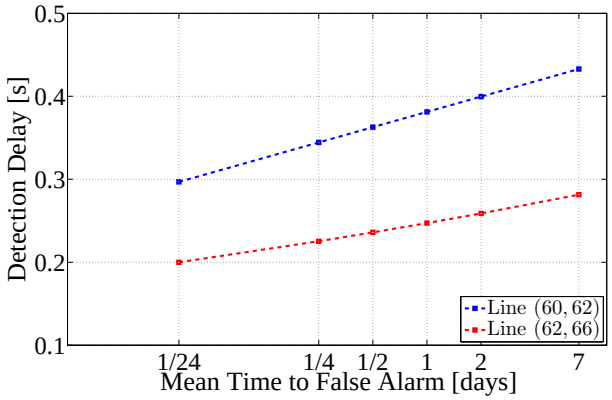

Figure 5.7: 118-bus system: Average Detection Delay vs. Mean Time to False Alarm.

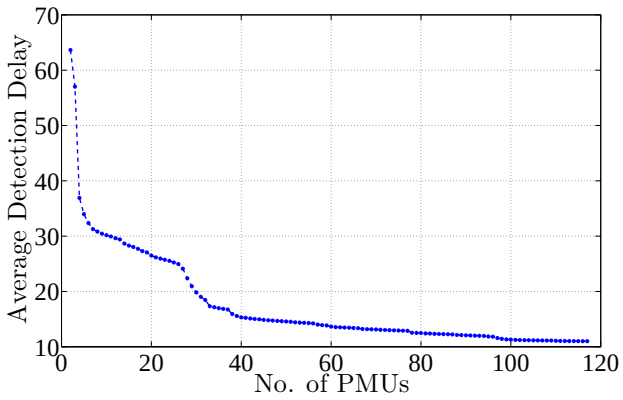

Figure 5.8: 118-bus system: Average Detection Delay vs. PMUs.

value obtained from exhaustive search.

5.5 Summary

This chapter provided several extensions of the basic QCD-based algorithm presented earlier. We partitioned the power system into multiple areas and applied the QCD-based algorithms in parallel for each area. A method to determine the optimal PMU allocation for each area was also presented. It was shown that both of these extensions can be formulated as an optimization program.

CHAPTER 6

CONCLUDING REMARKS

In this chapter we provide a summary of this thesis, highlight its main contributions, and conclude with some discussion of directions for future work.

6.1 Thesis Summary

This thesis is composed of six chapters. A framework for line outage detection exploiting the statistical properties of the voltage phase angle measurements is proposed. The methods developed within this framework are compared against other existing line outage detection methods and we show that our method is capable of real-time detection with better performance.

Chapter 2. This chapter provided the preliminary background of this research along with the statement of the problem to be addressed. The power system model was introduced; then, the linear incremental model was derived. Using this system model, we developed the pre- and post-outage statistical model of the voltage phase angles and presented the problem statement of quickest change detection.

Chapter 3. This chapter introduced the QCD-based line outage identification algorithms and the KL divergence, which is an important measure for characterizing the performance of these detection algorithms. Various other algorithms for line outage detection that exist in the literature were presented. Finally, we compared the performance of our proposed method against the other algorithms and showed that the CuSum-based method is better.

Chapter 4. In this chapter, an extension of the line outage algorithm proposed in Chapter 3 was presented. The new algorithm accounts for the transient dynamics that occur following a line outage. To model the transient behavior, participation factors were used to relate the active power gener-

ation to the load demand. The new algorithm was shown to have better performance compared to existing line outage detection algorithms and the algorithm proposed in Chapter 3, where the system transient dynamics are not considered.

Chapter 5. In this chapter, various extensions of the basic QCD-based algorithm were presented. The idea of partitioning the power system into multiple areas and applying the QCD-based algorithms in parallel for better scalability was introduced. In addition, for cases where PMUs are limited, a method to determine the optimal PMU allocation for each area was proposed.

6.2 Conclusion

This thesis provided a framework for line outage detection in power systems, which is crucial for maintaining operational reliability. Many of the current methods for online power system monitoring rely on a system model that can be inaccurate due to bad historical or telemetry data. These inaccuracies were a major factor in many blackouts. Therefore, there is a significant need for developing online techniques to detect and identify system topological changes.

The algorithm proposed in this thesis exploits fast measurements provided by PMUs and uses a statistical method to quickly detect network topological changes. The results of the proposed method are compared against the other line outage detection algorithms in literature. Additionally, it would not be economical to place a PMU at every bus across the power network. Therefore, we also consider the problem of optimal PMU placement at strategic locations for line outage detection.

6.3 Future Work

There are several extensions to this current work that are left for future work. The current method is not capable of detecting double line outage; new techniques that allow for quick detection of double line outages would be beneficial. Specifically, in terms of optimal PMU placement, there exists room for improving the current greedy algorithm. The formulation of the

PMU placement problem could be cast as a convex optimization and then existing techniques can be used for solving it. Finally, the algorithms presented in this work could be applied to other event detection problems in power systems such as switching of capacitors and transformers.

APPENDIX A

DERIVATIONS

A.1 Extension of KL Divergence

We can extend the idea of KL Divergence to compute $\mathbb{E}_{f_2}\left[\log\left(\frac{f_1}{f_0}\right)\right]$, which provides a measure for false alarm rates.

$$\begin{aligned}
\mathbb{E}_{f_2}\left[\log\left(\frac{f_1}{f_0}\right)\right] &= \int f_2(x)\log\left(\frac{f_1(x)}{f_0(x)}\right)dx \\
&= \int f_2(x)\log(f_1(x))dx - \int f_2(x)\log(f_0(x))dx \\
&= \int f_2(x)\log\left(\frac{f_1(x)}{f_2(x)}\right)dx + \int f_2(x)\log\left(\frac{f_2(x)}{f_0(x)}\right)dx \\
&= D(f_2 \parallel f_0) - D(f_2 \parallel f_1).
\end{aligned}$$

A.2 KL Divergence for Multivariate Gaussians

The KL Divergence between two Multivariate Gaussian variables can be computed analytically. Let $f_0 \sim \mathcal{N}(\mu_0, \Gamma_0)$ and $f_1 \sim \mathcal{N}(\mu_1, \Gamma_1)$ where $\Gamma_0, \Gamma_1 \in \mathbb{R}^{n\times n}$. Then,

$$
\begin{aligned}
D(f_1 \parallel f_0) &= \int f_1(x) \log\left(\frac{f_1(x)}{f_0(x)}\right) dx \\
&= \mathbb{E}_{f_1}\left[\log\left(\frac{f_1}{f_0}\right)\right] \\
&= \frac{1}{2}\log\left(\frac{\det\,\Gamma_0}{\det\,\Gamma_1}\right) \\
&\qquad + \frac{1}{2}\mathbb{E}_{f_1}\left[(x-\mu_0)^T\Sigma_0^{-1}(x-\mu_0) - (x-\mu_1)^T\Sigma_1^{-1}(x-\mu_1)\right] \\
&= \frac{1}{2}\log\left(\frac{\det\,\Gamma_0}{\det\,\Gamma_1}\right) + \frac{1}{2}\left[(\mu_1-\mu_0)^T\Sigma_0^{-1}(\mu_1-\mu_0) + \mathrm{Tr}(\Gamma_0^{-1}\Gamma_1)\right] - \frac{n}{2},
\end{aligned}
$$

where in the last step, we used the following identity [39]:

$$
\mathbb{E}\left[(x-c)^T A(x-c)\right] = (\mu-c)^T A(\mu-c) + \mathrm{Tr}(A\Gamma)
$$

for $x \sim \mathcal{N}(\mu, \Gamma)$.

APPENDIX B

DYNAMIC CUSUM

Assume a random process $\{X_k\}_{k=1}^{\infty}$ with the following statistical behavior:

$$X_k \sim \begin{cases} f_0, \text{ if } 1 \leq k < \gamma_0, \\ f^{(0)}, \text{ if } \gamma_0 \leq k < \gamma_1, \\ \vdots \\ f^{(i)}, \text{ if } \gamma_i \leq k < \gamma_{i+1}, \\ \vdots \\ f^{(T)}, \text{ if } \gamma_T \leq k, \end{cases} \tag{B.1}$$

where $\gamma_i \in \mathbb{N}$, $i = 0, \ldots, T$. The goal is to design a stopping rule that will detect the change in the statistical behavior of the observed process that takes place at time instant γ_0.

A heuristic test solution can be derived by considering this problem as a dynamic composite hypothesis testing problem. Thus, at every time instant k, choose between the following two hypotheses:

$$\begin{aligned} \mathrm{H}_0^k &: k < \gamma_0, \\ \mathrm{H}_1^k &: k \geq \gamma_0. \end{aligned}$$

The nominal hypothesis H_0^k corresponds to the case that the time instant γ_0 has not been crossed yet, while the alternative hypothesis H_1^k corresponds to the case that we have crossed γ_0. Each hypothesis induces a different set of distributions on the data $X_1, X_2, \ldots, X_k$. In particular, H_0^k is a single hypothesis under which the data follow distribution f_0 i.i.d. and H_1^k is a composite hypothesis, i.e., it induces one distribution belonging to a set of distributions. The distribution that is induced depends on the values of the γ's and k. To find the test statistic we first form the likelihood ratio of this

hypothesis testing problem for an arbitrary choice of γ's:

$$\frac{\prod_{j=\gamma_0}^{\min\{\gamma_1-1,k\}} f^{(0)}(X_j)\cdots \prod_{j=\min\{\gamma_T-1,k\}+1}^{k} f^{(T)}(X_j)}{\prod_{j=\gamma_0}^{k} f_0(X_j)}.$$

This likelihood ratio should be interpreted with the understanding that $\prod_{j=k+1}^{k} \frac{f^{(i)}(X_j)}{f_0(X_j)} \coloneqq 1$ for $i = 0, \ldots, T$. This is a natural generalization of the maximum likelihood interpretation of the CuSum statistic [21]. The test statistic is derived by taking the maximum with respect to $\gamma_0, \ldots, \gamma_T$. An equivalent test statistic can be derived by maximizing the logarithm of the above quantity. As a result, we have that

$$W[k] = \max_{\gamma_0<\cdots<\gamma_T} \left\{ \sum_{j=\gamma_0}^{\min\{\gamma_1-1,k\}} \log \frac{f^{(0)}(X_j)}{f_0(X_j)} + \ldots + \sum_{j=\min\{\gamma_T-1,k\}+1}^{k} \log \frac{f^{(T)}(X_j)}{f_0(X_j)} \right\}, \tag{B.2}$$

with the understanding that in $\gamma_0 \leq k$ holds. The expression in (B.2) can be written in the following way:

$$W[k] = \max\{\Omega^{(0)}[k], \ldots, \Omega^{(i)}[k], \ldots, \Omega^{(T)}[k]\}, \tag{B.3}$$

where

$$\Omega^{(i)}[k] = \max_{\gamma_0<\gamma_1<\cdots<\gamma_i\leq k} \left\{ \sum_{j=\gamma_0}^{\gamma_1-1} \log \frac{f^{(0)}(X_j)}{f_0(X_j)} + \ldots + \sum_{j=\gamma_i}^{k} \log \frac{f^{(i)}(X_j)}{f_0(X_j)} \right\}, i = 0, \ldots, T, \tag{B.4}$$

and using the fact that $\sum_{j=k+1}^{k} \log \frac{f^{(i)}(X_k)}{f_0(X_k)} = 1$, $i \in \{0, \ldots T\}$. We claim that the above expression can be written in a recursive manner as follows:

$$\Omega^{(i)}[k] = \max\{\Omega^{(i)}[k-1], \Omega^{(i-1)}[k-1]\} + \log \frac{f^{(i)}(X_k)}{f_0(X_k)},$$

for $i = 0, \ldots, T$ and $\Omega^{(0)}[k] \coloneqq 0$ for all $k \in \mathbb{Z}$. First, consider the case $i = 0$:

$$\begin{aligned}
\Omega^{(0)}[k] &= \max_{\gamma_0 \leq k} \left\{ \sum_{j=\gamma_0}^{k} \log \frac{f^{(0)}(X_j)}{f_0(X_j)} \right\} \\
&= \max_{\gamma_0 \leq k} \left\{ \sum_{j=\gamma_0}^{k-1} \log \frac{f^{(0)}(X_j)}{f_0(X_j)} + \log \frac{f^{(0)}(X_k)}{f_0(X_k)} \right\} \\
&= \max_{\gamma_0 \leq k} \left\{ \sum_{j=\gamma_0}^{k-1} \log \frac{f^{(0)}(X_j)}{f_0(X_j)} \right\} + \log \frac{f^{(0)}(X_k)}{f_0(X_k)} \\
&= \max \left\{ \max_{\gamma_0 \leq k-1} \left[\sum_{j=\gamma_0}^{k-1} \log \frac{f^{(0)}(X_j)}{f_0(X_j)} \right], \right. \\
&\qquad \left. \sum_{j=k}^{k-1} \log \frac{f^{(0)}(X_j)}{f_0(X_j)} \right\} + \log \frac{f^{(0)}(X_k)}{f_0(X_k)} \\
&= \max\{\Omega^{(0)}[k-1], 0\} + \log \frac{f^{(0)}(X_k)}{f_0(X_k)}.
\end{aligned}$$

Since $\Omega^{(-1)}[k] \coloneqq 0$, the argument we attempt to prove holds for the case of $i = 0$. Now for the case of an arbitrary i:

$$\begin{aligned}
\Omega^{(i)}[k] &= \max_{\gamma_0 < \gamma_1 < \cdots < \gamma_i \leq k} \left\{ \sum_{j=\gamma_0}^{\gamma_1 - 1} \log \frac{f^{(0)}(X_j)}{f_0(X_j)} + \ldots \right. \\
&\qquad \left. + \sum_{j=\gamma_i}^{k} \log \frac{f^{(i)}(X_j)}{f_0(X_j)} \right\} \\
&= \max_{\gamma_0 < \gamma_1 < \cdots < \gamma_i \leq k} \left\{ \sum_{j=\gamma_0}^{\gamma_1 - 1} \log \frac{f^{(0)}(X_j)}{f_0(X_j)} + \ldots \right. \\
&\qquad \left. + \sum_{j=\gamma_i}^{k-1} \log \frac{f^{(i)}(X_j)}{f_0(X_j)} \right\} + \log \frac{f^{(i)}(X_k)}{f_0(X_k)}.
\end{aligned}$$

Consider the first term of this expression. We have that:

$$\begin{aligned}
&\max_{\gamma_0<\gamma_1<\cdots<\gamma_i\leq k}\Bigg\{\sum_{j=\gamma_0}^{\gamma_1-1}\log\frac{f^{(0)}(X_j)}{f_0(X_j)}+\ldots\\
&+\sum_{j=\gamma_i}^{k-1}\log\frac{f^{(i)}(X_j)}{f_0(X_j)}\Bigg\}\\
&=\max\Bigg\{\max_{\gamma_0<\gamma_1<\cdots<\gamma_i\leq k-1}\Bigg[\sum_{j=\gamma_0}^{\gamma_1-1}\log\frac{f^{(0)}(X_j)}{f_0(X_j)}+\ldots\\
&+\sum_{j=\gamma_i}^{k-1}\log\frac{f^{(i)}(X_j)}{f_0(X_j)}\Bigg]\\
&=\max_{\gamma_0<\gamma_1<\cdots<\gamma_{i-1}\leq k-1}\Bigg[\sum_{j=\gamma_0}^{\gamma_1-1}\log\frac{f^{(0)}(X_j)}{f_0(X_j)}+\ldots\\
&+\sum_{j=\gamma_{i-1}}^{k-1}\log\frac{f^{(i-1)}(X_j)}{f_0(X_j)}\Bigg]\Bigg\}\\
&=\max\{\Omega^{(i)}[k-1],\Omega^{(i-1)}[k-1]\}.
\end{aligned}$$

It can be shown than an equivalent test arises if we force the Ω statistics to be non-negative. Thus, the D-CuSum test statistic is defined as follows:

$$W[k]=\max\Big\{\Omega^{(0)}[k],\ldots,\Omega^{(T)}[k]\Big\},\tag{B.5}$$

where

$$\begin{aligned}
\Omega^{(i)}[k]=\max\Bigg\{&\max\{\Omega^{(i)}[k-1],\Omega^{(i-1)}[k-1]\}+\\
&\log\frac{f^{(i)}(X[k])}{f_0(X[k])},0\Bigg\},i=0,\ldots,T,
\end{aligned}\tag{B.6}$$

where $\Omega^{(-1)}[k]\coloneqq 0$ for all $k\in\mathbb{Z}$ and $\Omega^{(i)}[0]\coloneqq 0$ for all i.

The corresponding stopping time is given by comparing $W[k]$ against a pre-determined positive threshold:

$$\tau=\inf\{k\geq 1:W[k]>A\}.$$

REFERENCES

[1] FERC and NERC, "Arizona-southern California outages on September 8, 2011: Causes and recommendations," Apr. 2012. [Online]. Available: http://www.ferc.gov.

[2] U.S.-Canada Power System Outage Task Force, "Final report on the August 14th blackout in the United States and Canada: causes and recommendations," Apr. 2004. [Online]. Available: http://energy.gov.

[3] K. A. Clements and P. W. Davis, "Detection and identification of topology errors in electric power systems," *IEEE Transactions on Power Systems*, vol. 3, no. 4, pp. 1748–1753, 1988.

[4] F. F. Wu and W. E. Liu, "Detection of topology errors by state estimation," *IEEE Transactions on Power Systems*, vol. 4, no. 1, pp. 176–183, 1989.

[5] L. Zhao and W. Song, "Distributed power-line outage detection based on wide area measurement system," *Sensors*, vol. 14, no. 7, p. 13114, 2014. [Online]. Available: http://www.mdpi.com/1424-8220/14/7/13114

[6] N. Singh and H. Glavitsch, "Detection and identification of topological errors in online power system analysis," *IEEE Transactions on Power Systems*, vol. 6, no. 1, pp. 324–331, 1991.

[7] F. Alvarado, "Determination of external system topology errors," *IEEE Transactions on Power Apparatus and Systems*, vol. PAS-100, no. 11, pp. 4553–4561, 1981.

[8] J. E. Tate and T. J. Overbye, "Line outage detection using phasor angle measurements," *IEEE Transactions on Power Systems*, vol. 23, no. 4, pp. 1644–1652, 2008.

[9] H. Zhu and G. B. Giannakis, "Sparse overcomplete representations for efficient identification of power line outages," *IEEE Transactions on Power Systems*, vol. 27, no. 4, pp. 2215–2224, 2012.

[10] H. Sehwail and I. Dobson, "Locating line outages in a specific area of a power system with synchrophasors," in *North American Power Symposium*, Sept 2012, pp. 1–6.

[11] R. Emami and A. Abur, "External system line outage identification using phasor measurement units," *IEEE Transactions on Power Systems*, vol. 28, no. 2, pp. 1035–1040, 2013.

[12] M. Garcia, T. Catanach, S. V. Wiel, R. Bent, and E. Lawrence, "Line outage localization using phasor measurement data in transient state," *IEEE Transactions on Power Systems*, vol. 31, no. 4, pp. 3019–3027, July 2016.

[13] Y. C. Chen, T. Banerjee, A. D. Domínguez-García, and V. V. Veeravalli, "Quickest line outage detection and identification," *IEEE Transactions on Power Systems*, vol. 31, no. 1, pp. 749–758, 2016.

[14] T. Banerjee, Y. C. Chen, A. D. Domínguez-García, and V. V. Veeravalli, "Power system line outage detection and identification—a quickest change detection approach," in *Proc. of the IEEE International Conference on Acoustics, Speech, and Signal Processing*, May 2014.

[15] H. V. Poor and O. Hadjiliadis, *Quickest Detection*. Cambridge University Press, 2009.

[16] R. Nuqui and A. Phadke, "Phasor measurement unit placement techniques for complete and incomplete observability," *IEEE Transactions on Power Delivery*, vol. 20, no. 4, pp. 2381–2388, Oct 2005.

[17] B. Milosevic and M. Begovic, "Nondominated sorting genetic algorithm for optimal phasor measurement placement," *IEEE Transactions on Power Systems*, vol. 18, no. 1, pp. 69–75, Feb 2003.

[18] M. Hajian, A. M. Ranjbar, T. Amraee, and B. Mozafari, "Optimal placement of PMUs to maintain network observability using a modified BPSO algorithm," *Int. J. Elect. Power Energy Syst.*, vol. 33, no. 1, pp. 28–34, Jan. 2011.

[19] Y. Zhao, A. Goldsmith, and H. Poor, "On pmu location selection for line outage detection in wide-area transmission networks," in *Power and Energy Society General Meeting, 2012 IEEE*, July 2012, pp. 1–8.

[20] N. Manousakis, G. Korres, and P. Georgilakis, "Taxonomy of PMU placement methodologies," *IEEE Transactions on Power Systems*, vol. 27, no. 2, pp. 1070–1077, May 2012.

[21] V. V. Veeravalli and T. Banerjee, *Quickest Change Detection*. Elsevier: E-reference Signal Processing, 2013.

[22] A. R. Bergen and V. Vittal, *Power Systems Analysis*. Prentice Hall, 2000.

[23] M. Lotfalian, R. Schlueter, D. Idizior, P. Rusche, S. Tedeschi, L. Shu, and A. Yazdankhah, "Inertial, governor, and AGC/economic dispatch load flow simulations of loss of generation contingencies," *IEEE Transactions on Power Apparatus and Systems*, vol. PAS-104, no. 11, pp. 3020 –3028, Nov. 1985.

[24] R. A. Horn and C. R. Johnson, *Matrix Analysis*. Cambridge University Press, 1985.

[25] B. Hajek, *Random Processes for Engineers*. Cambridge University Press, 2015.

[26] A. G. Tartakovsky, I. V. Nikiforov, and M. Basseville, *Sequential Analysis: Hypothesis Testing and Change-Point Detection*, ser. Statistics. CRC Press, 2014.

[27] M. Pollak, "Optimal detection of a change in distribution," *Ann. Statist.*, vol. 13, no. 1, pp. 206–227, Mar. 1985.

[28] T. L. Lai, "Information bounds and quick detection of parameter changes in stochastic systems," *IEEE Trans. Inf. Theory*, vol. 44, no. 7, pp. 2917–2929, Nov. 1998.

[29] G. Fellouris and G. Sokolov, "Second-order asymptotic optimality in multisensor sequential change detection," October 2014, http://arxiv.org/abs/1410.3815v2. [Online]. Available: http://arxiv.org/abs/1410.3815v2

[30] A. G. Tartakovsky and A. S. Polunchenko, "Quickest changepoint detection in distributed multisensor systems under unknown parameters," in *Proc. of IEEE International Conference on Information Fusion*, July 2008, pp. 1–8.

[31] "Power system test case archive," Oct. 2012. [Online]. Available: http://www.ee.washington.edu/research/pstca.

[32] R. D. Zimmerman, C. E. Murillo-Sanchez, and R. J. Thomas, "Matpower: Steady-state operations, planning and analysis tools for power systems research and education," *IEEE Transactions on Power Systems*, vol. 26, no. 1, pp. 12–19, Feb. 2011.

[33] G. Rovatsos, X. Jiang, A. D. Domínguez-García, and V. V. Veeravalli, "Comparison of statistical algorithms for power system line outage detection," in *Proc. of the IEEE International Conference on Acoustics, Speech, and Signal Processing*, Apr. 2016.

[34] P. Elias, "Error-correcting codes for list decoding," *IEEE Transactions on Information Theory*, vol. 37, no. 1, pp. 5–12, Jan 1991.

[35] J. Chow and K. Cheung, "A toolbox for power system dynamics and control engineering education and research," *IEEE Transactions on Power Systems*, vol. 7, no. 4, pp. 1559–1564, Nov. 1992.

[36] D. Ramsden, "Optimization approaches to sensor placement problems," Ph.D. dissertation, Rensselaer Polytechnic Institute, 2009.

[37] J. P. Hespanha, "`grPartition` a MATLAB function for graph partitioning," Available at http://www.ece.ucsb.edu/ hespanha, Oct. 2004.

[38] G. Karypis and V. Kumar, "Multilevel k-way partitioning scheme for irregular graphs," *Journal of Parallel and Distributed Computing*, vol. 48, no. 1, pp. 96–129, 1998.

[39] K. B. Petersen and M. S. Pedersen, "The matrix cookbook," 2012. [Online]. Available: http://matrixcookbook.com